6-14-2003

Phytoplankton Response to Intrusions of Slope Water on the West Florida Shelf: Models and Observations

John J. Walsh
University of South Florida, jwalsh@usf.edu

Robert H. Weisberg
University of South Florida, weisberg@usf.edu

Dwight A. Dieterle
University of South Florida

Ruoying He
University of South Florida

Brian P. Darrow
University of South Florida

See next page for additional authors

Phytoplankton response to intrusions of slope water on the West Florida Shelf: Models and observations

John J. Walsh,[1] Robert H. Weisberg,[1] Dwight A. Dieterle,[1] Ruoying He,[1] Brian P. Darrow,[1] Jason K. Jolliff,[1] Kristen M. Lester,[1] Gabriel A. Vargo,[1] Gary J. Kirkpatrick,[2] Kent A. Fanning,[1] Tracey T. Sutton,[1] Ann E. Jochens,[3] Douglas C. Biggs,[3] Bisman Nababan,[1] Chuanmin Hu,[1] and Frank E. Muller-Karger[1]

Received 25 March 2002; revised 6 December 2002; accepted 6 February 2003; published 14 June 2003.

[1] Previous hypotheses had suggested that upwelled intrusions of nutrient-rich Gulf of Mexico slope water onto the West Florida Shelf (WFS) led to formation of red tides of *Karenia brevis*. However, coupled biophysical models of (1) wind- and buoyancy-driven circulation, (2) three phytoplankton groups (diatoms, *K. brevis*, and microflagellates), (3) these slope water supplies of nitrate and silicate, and (4) selective grazing stress by copepods and protozoans found that diatoms won in one 1998 case of no light limitation by colored dissolved organic matter (CDOM). The diatoms lost to *K. brevis* during another CDOM case of the models. In the real world, field data confirmed that diatoms were indeed the dominant phytoplankton after massive upwelling in 1998, when only a small red tide of *K. brevis* was observed. Over a 7-month period of the CDOM-free scenario the simulated total primary production of the phytoplankton community was $\sim$1.8 g C m^{-2} d^{-1} along the 40-m isobath of the northern WFS, with the largest accumulation of biomass on the Florida Middle Ground (FMG). Despite such photosynthesis, these models of the WFS yielded a net source of CO_2 to the atmosphere during spring and summer and suggested a small sink in the fall. With diatom losses of 90% of their daily carbon fixation to herbivores the simulation supported earlier impressions of a short, diatom-based food web on the FMG, where organic carbon content of the surficial sediments is tenfold those of the surrounding seabeds. Farther south, the simulated near-bottom pools of ammonium were highest in summer, when silicon regeneration was minimal, leading to temporary Si limitation of the diatoms. Termination of these upwelled pulses of production by diatoms and nonsiliceous microflagellates mainly resulted from nitrate exhaustion in the model, however, mimicking most del^{15}PON observations in the field. Yet, the CDOM-free case of the models failed to replicate the observed small red tide in December 1998, tagged with the del^{15}N signature of nitrogen fixation. A large red tide of *K. brevis* did form in the CDOM-rich case, when estuarine supplies of CDOM favored the growth of the shade-adapted, ungrazed dinoflagellates. The usual formation of large harmful algal blooms of >1 ug chl L^{-1} (10^5 cells L^{-1}) in the southern part of the WFS, between Tampa Bay and Charlotte Harbor, must instead depend upon local aeolian and estuarine supplies of nutrients and CDOM sun screen, not those from the shelf break. In the absence of slope water supplies, local upwelling instead focuses nitrate-poor innocula of co-occurring *K. brevis* and nitrogen fixers at coastal fronts for both aggregation and transfer of nutrients between these phytoplankton groups. *INDEX TERMS:* 4255 Oceanography: General: Numerical modeling; 4279 Oceanography: General: Upwelling and convergences; 4815 Oceanography: Biological and Chemical: Ecosystems, structure and dynamics; 4855 Oceanography: Biological and Chemical: Plankton; 4880 Oceanography: Biological and Chemical: Trophodynamics; *KEYWORDS:* predicting redtides, West Florida Shelf ecology

Citation: Walsh, J. J., et al., Phytoplankton response to intrusions of slope water on the West Florida Shelf: Models and observations, *J. Geophys. Res.*, *108*(C6), 3190, doi:10.1029/2002JC001406, 2003.

[1]College of Marine Science, University of South Florida, St. Petersburg, Florida, USA.
[2]Mote Marine Laboratory, Sarasota, Florida, USA.
[3]Department of Oceanography, Texas A&M University, College Station, Texas, USA.

0148-0227/03/2002JC001406

1. Introduction

[2] Background nitrate levels of <0.1 umol NO_3 kg^{-1} on the oligotrophic West Florida Shelf (WFS) suggested that the initiation of red tides of *Karenia brevis* might be attributed to upwelled supplies of nutrient-rich Loop Cur-

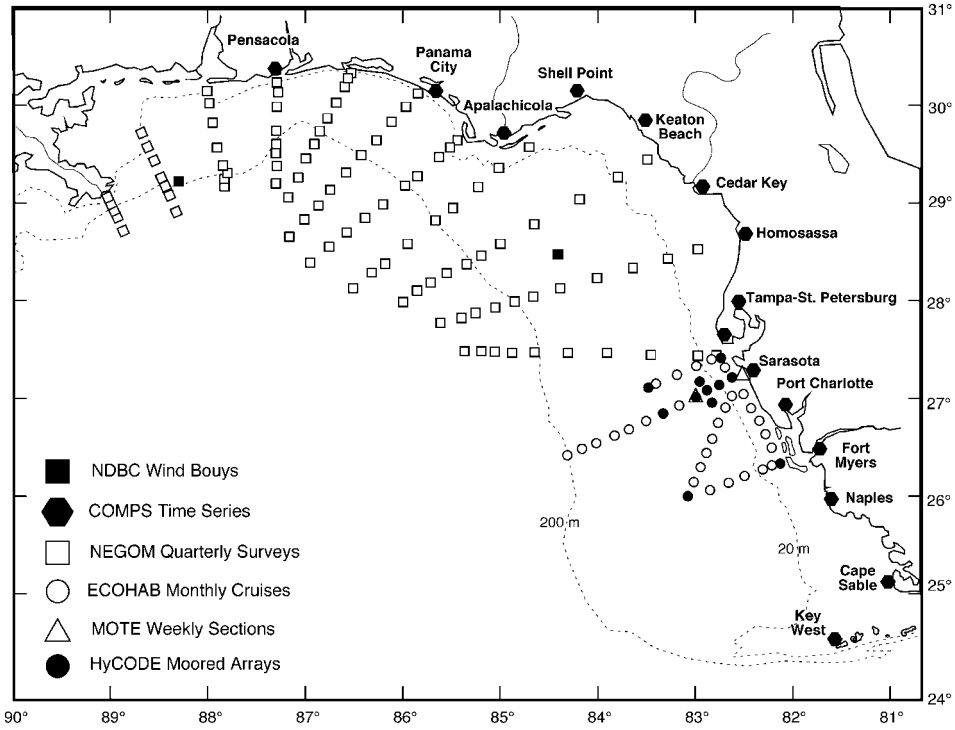

Figure 1. Station locations of the ECOHAB (open circles), MOTE (open triangles), and NEGOM (open squares) surveys of the West Florida Shelf in relation to HyCODE current meter moorings (solid circles), COMPS sea level gauges (solid hexagons), and NDBC wind buoys (solid squares) during March 1998 to December 1999.

rent water [*Haddad and Carder*, 1979; *Tester and Steidinger*, 1997]. However, our prior analysis of upwelling events that penetrated to the 40-m isobath of the WFS during 1958–1961 found no associated biomass increments of *K. brevis* [*Walsh and Steidinger*, 2001]. The outcome of competition among those phytoplankton populations was then unknown, since only cell counts of the toxic dinoflagellate were made. Using a numerical model of three phytoplankton groups of diatoms, flagellates, and *K. brevis*, subjected to selective grazing stress by copepods and protozoans, the algal community's response to slope water nutrient supplies, induced by wind and buoyancy forcings, was thus examined during 7 months of 1998, when validation data were obtained.

[3] As part of our NOAA/EPA ECOHAB (Ecology and Oceanography of Harmful Algal Blooms) study, a series of 17 cross-shelf sections were taken off Sarasota, FL during March 1998 to February 1999 (Figure 1), involving measurements of temperature, salinity, nutrients (NO_3, NO_2, NH_4, PO_4, SiO_4, Fe, DOP, DON), O_2, chlorophyll, phaeopigments, PON, POC, POP, CDOM fluorescence/absorption, and the dominant species of phytoplankton and zooplankton. Additional data were collected here during June, August, and September 1998 as part of the ONR HyCODE (Hyperspectral Coastal Ocean Dynamics Experiment) program. Farther to the north, quarterly surveys of the MMS NEGOM (Northeastern Gulf of Mexico) project provided the upstream conditions across 11 other sections during May, July–August, and November 1998.

[4] Since nitrogen fixation by co-occurring *Trichodesmium* may be another source of "new" nitrogen for WFS red tides [*Walsh and Steidinger*, 2001; *Lenes et al.*, 2001], the del^{15}N of PON was also measured on the ECOHAB cruises. In prior field studies of water parcels shed by a western boundary current, the temporal change of the ^{15}N content of phytoplankton PON was attributed to less fractionation during their uptake of smaller amounts of available nitrate [*Altabet and McCarthy*, 1985]. During the initial process of nitrate or ammonium uptake, the algae discriminate against ^{15}N such that the del^{15}N of their PON, where del^{15}N(‰) = {(^{15}N/^{14}N)/(air standard) − 1} 1000, is smaller than the nitrogen source after their assimilation of ^{14}N.

[5] If we consider an upwelled parcel of slope water to be a closed system, as it drifts onshore toward the west coast of Florida, the final del^{15}N of phytoplankton PON should be that of the initial dissolved stocks, after uptake of the progressively enriched ^{15}N of nitrate left behind in the water column [*Mariotti et al.*, 1981]. The upstream western boundary current that becomes the Loop Current after passage through Yucatan Straits has a range of del$^{15}NO_3$ values, from +6.7‰ to +8.3‰ over depths of 200–500 m on the Venezuelan slope [*Liu and Kaplan*, 1989], such that WFS phytoplankton grown on nitrate-depleted Loop Current water might have a similar del^{15}PON. We base this assumption on identical relationships of temperature, salinity, and nitrate within the aphotic zones of the NEGOM study in the Gulf of Mexico [*Jochens and Nowlin*, 1999] and the WOCE study of the southern Caribbean Sea [*Weisberg and He*, 2003]. In contrast, *Trichodesmium* has a del^{15}PON of −0.8‰ [*Minagawa and Wada*, 1986].

[6] During spring 1998, 'anomalous' west winds (Figure 2) led to strong upwelling along the Florida Panhandle

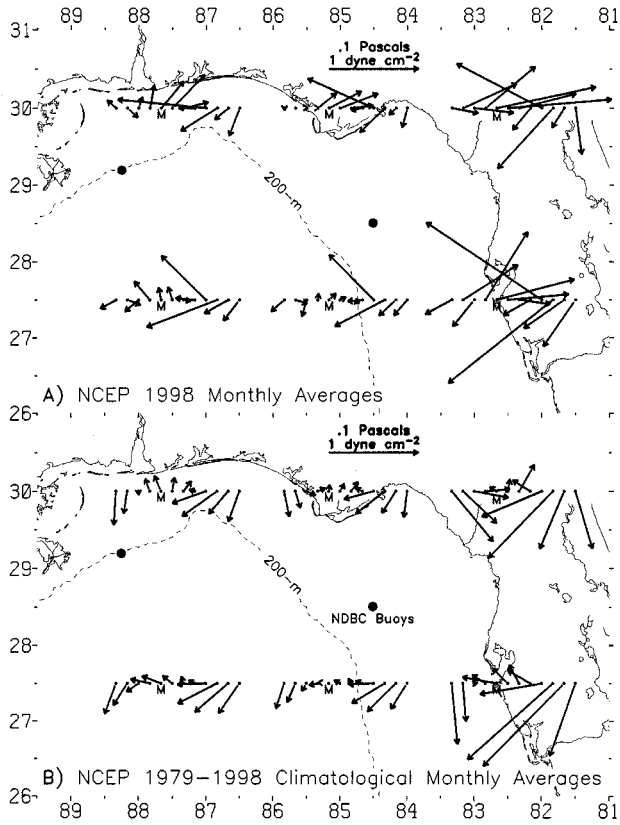

Figure 2. Spatial patterns of wind stresses (dynes cm^{-2}) used to force (a) 1998 upwelling events of varying intensity in relation to (b) the 20-year climatological mean during 1979–1998 and locations of NDBC buoys (solid circles) along the Panhandle and west coasts of Florida.

[*Muller-Karger*, 2000], such that the May 1998 sea surface temperatures near Pensacola, Florida, at the head of DeSoto Canyon (Figure 1), were 2°–4°C colder than either on the Alabama shelf at this time, or in the same region during May 1999. Consequently, the near-bottom isopleth of 1 umol NO_3 kg^{-1} penetrated to the ~20-m isobath in the Panhandle, Big Bend, and Southeastern regions of the WFS by May 1998 (Figure 3a). In contrast, a near-bottom stock of 1 umol NO_3 kg^{-1} was only found at the ~65-m isobath of these regions during May 1999, 2000, and 2001. Thus, at 16 stations on the 10–50-m isobaths between Apalachicola and Tampa Bays, the mean near-bottom stock was 3.13 umol NO_3 kg^{-1} in May 1998, compared to 0.11 umol NO_3 kg^{-1} in May 1999 (Table 1). In an ecological model, coupled to the three-dimensional Princeton Ocean Model [*Weisberg and He*, 2003], we simulated the phytoplankton response to such nitrate-rich intrusions during May, September, and October/November 1998 (Figure 4b).

2. Methods

2.1. Observations

[7] Cross-shelf ECOHAB sections were taken along the Sarasota line past five HyCODE ADCP arrays, moored on the 10, 20, 25, and 30, and 50-m isobaths (Figure 1), such that the temperature (Figure 4a) and salinity observations used in this analysis are from both the ADCP arrays and the CTD casts on discrete stations. At these hydrographic stations, micromolar levels of inorganic nutrients (NO_3, NO_2, PO_4, SiO_4) were determined with standard methods [*Atlas et al.*, 1971; *Gordon et al.*, 1994], while nanomolar

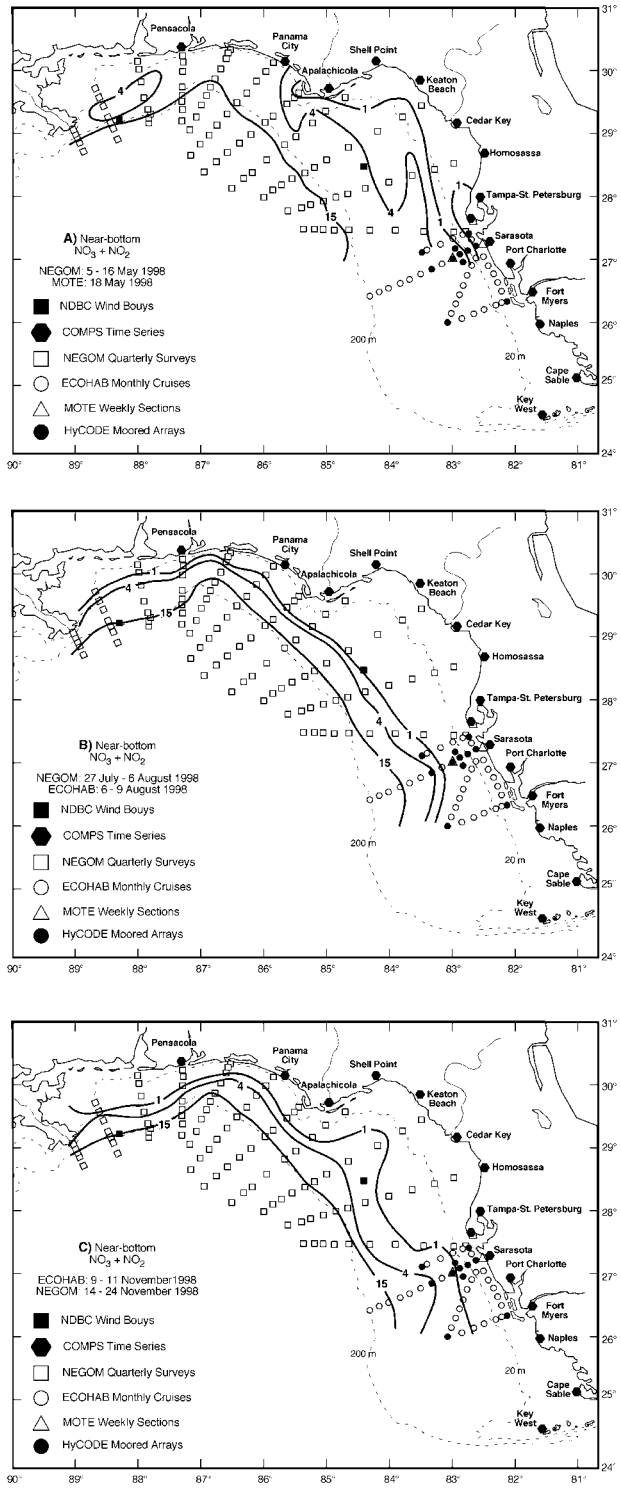

Figure 3. A seasonal composite of the near-bottom fields (μmol kg^{-1}) of nitrate + nitrite found by ECOHAB/NEGOM surveys of the West Florida Shelf during (a) spring, (b) summer, and (c) fall 1998.

Table 1. Mean Interannual and Seasonal Variation of Nutrient Pools in the Big Bend (BB) Region, Upstream of the ECOHAB Site on the West Florida Shelf, in Relation to del^{15}N (‰) of Surface Particulate Matter, Between Tampa Bay and Charlotte Harbor, During 1998/1999[a]

	Near-Surface (n = 25) BB Above the 10–200 m Isobaths	Near-Bottom (n = 16) BB Above the 10–50 m Isobaths	Surface ECOHAB (n = 6) Above the 10–50 m Isobaths
		May 1998/1999	
Nitrate + nitrite	0.17/0.12	3.13/0.11	. . .
Urea	0.17/0.12	3.13/0.11	. . .
Ammonium	0.13/0.09	0.39/0.12	. . .
Phosphate	0.04/0.04	0.20/0.05	. . .
Silicate	1.18/1.24	4.02/1.62	. . .
del^{15}PON	. . .	. . .	. . ./1.97[b]
		June 1998/1999	
del^{15}PON	. . .	. . .	. . ./8.32
		July 1998/1999	
del^{15}PON	. . .	. . .	7.95[c]/4.68
		August 1998/1999	
Nitrate + nitrite	0.13/0.14	0.48/0.13	. . .
Urea	0.19/0.09	0.21/0.09	. . .
Ammonium	0.16/0.13	0.20/0.18	. . .
Phosphate	0.05/0.04	0.11/0.06	. . .
Silicate	1.27/0.76	2.21/1.89	. . .
del^{15}PON	. . .	. . .	2.74[b]/3.79
		September 1998/1999	
del^{15}PON	. . .	. . .	9.17[c]/3.82
		October 1998/1999	
del^{15}PON	. . .	. . .	3.56[d]/4.97[e]
		November 1998/1999	
Nitrate + nitrite	0.16/0.09	0.75/0.19	. . .
Urea	0.09/0.13	0.07/0.09	. . .
Ammonium	0.07/0.06	0.15/0.11	. . .
Phosphate	0.03/0.04	0.06/0.04	. . .
Silicate	0.93/1.00	1.52/1.08	. . .
del^{15}PON	. . .	. . .	6.80[c]/3.03
		December 1998/1999	
del^{15}PON	. . .	. . .	5.81[e]/5.25

[a]Interannual and seasonal variation are in umol kg^{-1}, and del^{15}N are in per mil.
[b]Surface colonies of *Trichodesmium* had del^{15}N values of −0.82 to −0.57‰ in September and October 2000.
[c]A mean value of 7.97‰ within nitrate-depleted waters.
[d]del^{15}N values of 4.45 and 4.18‰ were found for blooms of diatoms near-bottom at the 30-m isobath and near-surface at the mouth of Tampa Bay in October 2000. *Rhizosolenia spp.* were a dominant group.
[e]Red tides of *Karenia brevis* had values of 3.63‰ at their chlorophyll biomass of ∼0.5 ug chl l^{-1} in October 2000, 4.37‰ at ∼1.0 ug chl l^{-1} in October 1999, 4.88‰ at ∼5.0 ug chl l^{-1} in December 1998, and 5.11‰ at ∼25.0 ug chl l^{-1} in October 2000, assuming a cellular content of 1×10^{-5} ug chl cell^{-1}.

levels of NO_3 and NO_2 were detected with a fluorescence technique [*Masserini and Fanning*, 2000]. To provide a consistent data set, we report the results of nitrate + nitrite measurements as umol NO_3 kg^{-1} (Figure 3). Urea was only measured on the NEGOM cruises [*Aminot and Kerovel*, 1982]. Ammonium, however, was again determined at micromolar [*Slawyk and MacIsaac*, 1972] and nanomolar [*Masserini and Fanning*, 2000] levels.

[8] CDOM (colored dissolved organic matter) fluorescence at 450 nm wavelength was measured in relation to underway conductivity and temperature data. Discrete estimates of CDOM absorption were obtained by spectrometric analyses of samples filtered through GF/F and 0.2 um nucleopore membrane filters [*Del Castillo et al.*, 2000; *Hu et al.*, 2003]. Satellite estimates of CDOM were also made with the MODIS algorithm [*Carder et al.*, 1999].

[9] Extracted chlorophyll stocks were measured with both the Holm-Hansen/Welschmeyer fluorometric protocols [*Heil et al.*, 2002] and HPLC assays [*Wright et al.*, 1991], which yielded similar estimates of the amount of chlorophyll *a*. These data were used to calibrate the ECOHAB and NEGOM underway maps (Figure 5) of surface chlorophyll fluorescence, with an r^2 of ∼0.90 [*Hu et al.*, 2003], which in turn calibrated satellite imagery. To save space, we refer the reader to the USF-archived time series of 1998 SeaWiFS color images, but highlight a critical finding on both contamination of the imagery and shading of phytoplankton competitors by CDOM.

[10] A comparison of the standard SeaWiFS estimate [*O'Reilly et al.*, 1998] of surface pigment stocks with the underway data (Figure 5) indicated as much as an approximately fivefold overestimate of phytoplankton biomass by

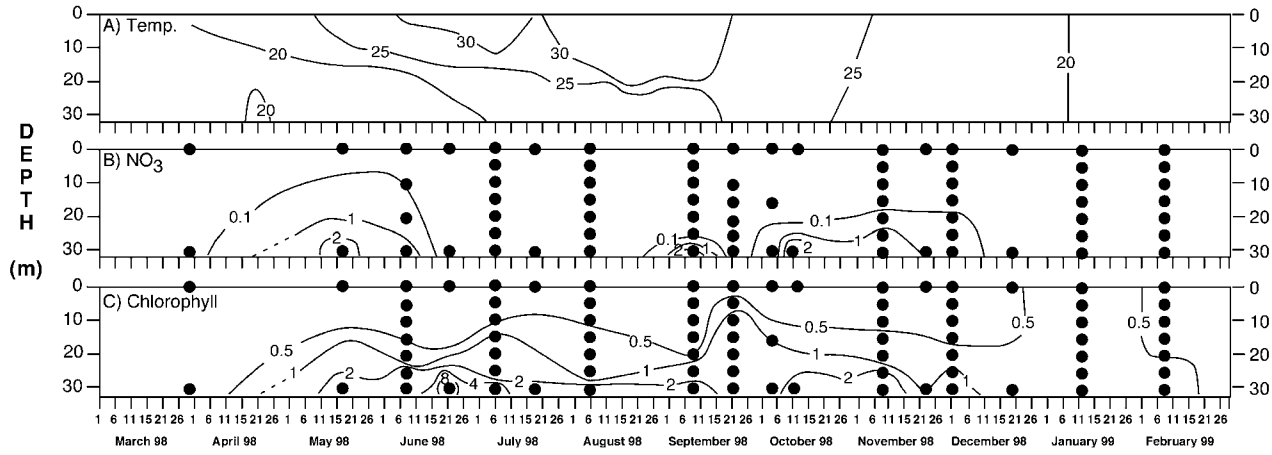

Figure 4. Yearlong time series of ECOHAB/MOTE observations of (a) temperature (°C), (b) nitrate + nitrite, and (c) chlorophyll above the 30-m isobath of the Sarasota line. See Figure 1 for location.

the satellite during May 1998, in contrast to little error during November 1998. A difference of ~4 ug chl L^{-1} in May [*Hu et al.*, 2003] and a bulk community specific attenuation coefficient at ~443 nm [*Gordon*, 1992] of 0.034 m^2 (mg chl)$^{-1}$, similar to two of the model's functional groups (Table 2), would yield a possible CDOM attenuation of ~0.136 m^{-1} on the WFS during spring 1998. At this time, the surface salinities within ~100 km of the coast were 3–4 psu lower than in May 1999, suggesting anomalous west winds both upwelled water and led to large freshwater runoff after the 1997–1998 El Nino [*Muller-Karger*, 2000].

[11] A larger CDOM value of 0.156 m^{-1} was measured at a salinity of 34.0 psu [*Hu et al.*, 2003], which was the mean salt content over a 10-m thick river plume, found over large areas of the WFS during August 1998 [*Jochens and Nowlin*, 1999]. With a cosine of the subsurface solar zenith angle of 0.82, such a CDOM attenuation coefficient of 0.190 m^{-1} would lead to an 85% loss of blue light within the upper 10 m of the water column. Phytoplankton utilization of the upwelled nutrients would then be severely light-limited, if estuarine CDOM were present, such that we considered two scenarios of the presence and absence of CDOM in the coupled models.

2.2. Ecological Model

[12] In the absence of much CDOM, a previous 1-dimensional [*Walsh et al.*, 2001] model of phytoplankton competition on the WFS found that diatoms won, when a simulated community of small and large diatoms, coccoid cyanophytes, nitrogen-fixing *Trichodesmium*, nontoxic and red tide dinoflagellates, microflagellates, and coccolithophores were subjected to estuarine and/or slope water supplies of nitrate. Thus they were our first choice of this 3-D study and the details of their niche, i.e., the parameter values of Table 2, are discussed in Appendix A.

[13] To evaluate a second hypothesis of delayed red tide initiation from near-bottom recycled nitrogen (Figure 6) after intrusions of slope water (note that mean stocks of both urea and ammonium were twofold to threefold higher in May 1998 than in May 1999 (Table 1)) the second phytoplankton variable of slow growing, dark-adapted, migratory *K. brevis* was allowed to harvest NH_4 at a greater affinity than the diatoms (Table 2).

[14] The mean NO_3/SiO_4 ratio of near-bottom slope waters at a depth of 200 m of the NEGOM stations was 2.0 (n = 98), such that after diatoms removed half of the nitrate, no silicate would be left. The near-bottom NO_3/PO_4 ratio at this shelf-break was instead a Refield one of ~16.6, ensuring additional growth of other phytoplankton within onwelled slope waters. Thus a third functional group of nanoplankton microflagellates was included in our model to reflect the background populations of nonsiliceous phytoplankton, identified from the HPLC analyses.

2.3. Numerical Experiments

[15] Our present application of the Princeton Ocean Model (POM) used ~2-km horizontal resolution and 21 vertical sigma layers over a curvilinear grid, extending from west of the Mississippi River to the Florida Keys. It was forced by wind stresses (Figure 2) and heat fluxes at the surface and by river inflows at the coast. The open boundary was sufficiently far from the shelf break to insure that the radiation conditions there did not impact the computed WFS flows.

[16] In the absence of an imposed Loop Current, however, vectors within the bottom Ekman layer of the POM were much slower than those observed [*Weisberg and He*, 2003]. Imposition of an offshore pressure distribution, in the form of sea level perturbation [*He and Weisberg*, 2003] along the open boundary, alleviated this problem. We thus used the POM, with and without the Loop Current, to drive the ecological model, with and without CDOM, in a series of numerical experiments over a period of ~215 days. Using the spring, summer, and fall NEGOM data on temperature, salinity, nutrients, and chlorophyll *a* as upstream boundary conditions across the Pensacola section (Figure 1), we computed the downstream distributions of u, v, w, K_z, T, S, PAR (z), NO_3, NH_4, SiO_4, chlorophyll biomass of diatoms, *K. brevis*, and flagellates, and carbon content of copepod and protozoan pellets under seasonal wind (Figure 2a) and freshwater forcings.

[17] The offshore boundary conditions of the biochemical variables were daily interpolations of the NEGOM and

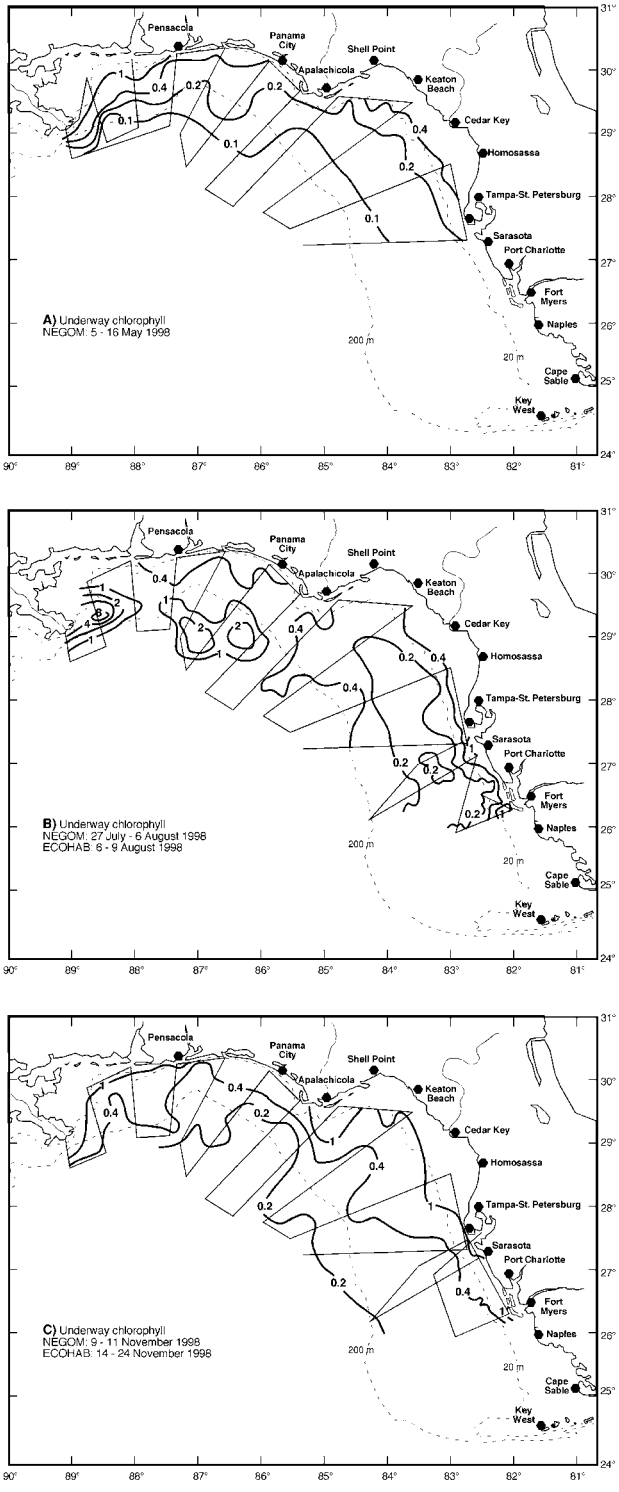

Figure 5. A seasonal composite of the surface chlorophyll fields ($\mu g\ L^{-1}$) found by the ECOHAB/NEGOM underway surveys of the West Florida Shelf during (a) spring, (b) summer, and (c) fall 1998.

ECOHAB data along the 200-m isobath. At the coast, we only added the interpolated daily estimates of buoyancy fluxes [*He and Weisberg*, 2002], and not the organic (CDOM) and inorganic nutrient supplies, from seven rivers (Mississippi, Mobile, Apalachicola, Suwannee, Hillsborough, Peace, and Shark) to the top sigma level of the grid cells adjacent to the shoreline [*Kourafalou et al.*, 1996]. The river inflows were thus climatological estimates, not those of 1998, such that any unusual low salinities and associated light-filtering CDOM in the POM were the result of advection and not due to interannual variations of freshwater loadings.

[18] Based upon ~120 nearshore measurements of CDOM absorption and salinity [*Del Castillo et al.*, 2000; *Hu et al.*, 2003], with an assumed spectral slope for CDOM of 0.020 nm^{-1}, we specified blue light attenuation of CDOM from POM's salinity field, SAL, at each grid point by

$$\begin{aligned} \mathrm{CDOM}(443) &= 3.470 - 0.095 \times \mathrm{SAL}; \mathrm{SAL} = 28.0 - 36.5 \\ &= 0.892 - 0.003 \times \mathrm{SAL}; \mathrm{SAL} = 24.0 - 28.0 \\ &= 2.250 - 0.060 \times \mathrm{SAL}; \mathrm{SAL} = 0.0 - 24.0 \end{aligned}$$

The Loop Current scenario of the POM included this CDOM forcing in the first case, while the absence of both Loop Current and CDOM constituted the second case. We thus ignored both photolysis and any sources of marine CDOM.

3. Results

3.1. Spring Shading: Shelf-Wide CDOM Export

3.1.1. Observations

[19] During March–May 1998, the wind field (Figure 2a) was anomalous, compared to the climatological state (Figure 2b), with persistent west, upwelling favorable winds along the Panhandle coast of Florida. Within the salinity maximum of ~36.6 at a depth of ~125 m in slope waters of DeSoto Canyon, the temperature during 12 May 1998 was ~19°C [*Jochens and Nowlin*, 1999], with nutrient stocks of 6.9 umol NO_3 kg^{-1}, 3.6 umol SiO_4 kg^{-1}, 0.34 umol PO_4 kg^{-1}, and an algal stock of ~0.08 ug chl L^{-1}. The urea and ammonium stocks were then each minimal at ~0.03 umol N kg^{-1}, compared to tenfold larger amounts on the shelf (Table 1).

[20] Similar hydrographic (36.6, ~19°C), reduced chemical (5.2 umol NO_3 kg^{-1}, 2.9 umol SiO_4 kg^{-1}, 0.27 umol PO_4 kg^{-1}), and higher phytoplankton (0.95 ug chl L^{-1}) values were found in bottom waters at the 45-m isobath off Sarasota during 9 June 1998. Using a diatom PN/chl ratio of 0.6 (C/chl ratio of Table 2 and Redfield C/N of 6.67), the biomass increment of 0.87 ug chl L^{-1} was equivalent to a depletion of 1.5 umol NO_3 kg^{-1} during transit. An initial concentration of 6.7 umol NO_3 kg^{-1} within this water parcel on the shelf would thus be about the same as that found at the salinity maximum within May slope waters, suggesting a recent intrusion of upwelled water, perhaps in May (Figure 3a), if not earlier.

[21] Within shallower waters of presumed greater light penetration, the initial algal stocks of <0.5 ug chl L^{-1} at the 30-m isobath in late March grew to 3.4 ug chl L^{-1} by 6 June and 10.6 ug chl L^{-1} on June 22 (Figure 4c), when <0.1 umol NO_3 kg^{-1} was found (Figure 4b). Note that the diatom PN/chl ratio of 0.6 and depletion of 6 umol NO_3 kg^{-1} would yield a near-bottom biomass of 10 ug chl L^{-1}, providing a consistent chemical mass balance for transit of an upwelled water parcel from a depth of ~125 m on the

Table 2. Model Parameters for Competition Among Diatoms, Microflagellates, and *K. brevis* [i = d, f, b]

Symbol	Parameter Value	Process
c_i	[0.275,0.225,0.100] $e^{.0693T}$	Maximum algal growth rate as a function of temperature, T, (d^{-1})
g_i		Realized algal growth rate as a function of light and nutrient (d^{-1})
$g_{i,\ NO_3}$		Realized uptake rate of nitrate (d^{-1})
$g_{i,\ NH_4}$		Realized uptake rate of ammonium (d^{-1})
$g_{i,\ SiO_4}$		Realized uptake rate of silicate (d^{-1})
L(t, z)		Photosynthetic active radiation (PAR) over time and depth (W m^{-2})
L_{is}	[43.2, 62.5, 14.8]	Saturation (optimal) light intensity for growth (W m^{-2})
I_m		Maximum noon radiation (W m^{-2})
I_p		Daily mean PAR (W m^2)
R_b	0.5	Fraction of surface PAR in the blue wavelength
t_s		Time since sunrise (hours)
Δ		Photoperiod (hours)
λ_d		Grazing rate on diatoms (umole C Kg^{-1} ind^{-1} d^{-1})
λ_b		Grazing rate on *K. brevis* (umole C Kg^{-1} ind^{-1} d^{-1})
G_d		Grazer abundance eating diatoms (ind m^{-3})
G_b		Grazer abundance eating *K. brevis* (ind m^{-3})
$\lambda_d G_d$	$0.7 g_d P_d$	Grazing pressure on diatoms (umole C Kg^{-1} d^{-1})
$\lambda_b G_b$	$0.005 g_b P_b$	Grazing pressure on *K. brevis* (umole C Kg^{-1} d^{-1})
Φ_f	0.030	uflagellate grazing pressure (umole C Kg^{-1} d^{-1})
w_d	$0.25 P_d$	Diatom sinking velocity (m d^{-1})
w_b	1.0	*K. brevis* migration velocity (m h^{-1})
w_{zd}	100.0	Sinking velocity of siliceous fecal pellets (m d^{-1})
w_{zf}	30.0	Sinking velocity of nonsiliceous fecal pellets (m d^{-1})
α_d	0.05	Remineralization rate of siliceous fecal pellets (d^{-1})
α_f	0.05	Remineralization rate of nonsiliceous fecal pellets (d^{-1})
β	0.01	Dissolution rate of particulate silicon (d^{-1})
ε_i	[0.85, 0.85, 0.85]	Fraction of grazed phytoplankton respired to DIC
k_{iNO_3}	[1.05, 0.20, 0.50]	Half-saturation constant for nitrate (umole N Kg^{-1})
k_{iNH_4}	[1.50, 0.20, 0.50]	Half-saturation constant for ammonium (umole N Kg^{-1})
k_{iSIO_4}	[1.15, 0.0, 0.0]	Half-saturation constant for silicate (umole Si Kg^{-1})
k_{NIT}	0.10	Half-saturation constant for nitrification (umole N Kg^{-1})
k_b	0.04	Attenuation coefficient for blue light at 443nm (m^{-1})
k_r	0.40	Attenuation coefficient for red light at 670 nm (m^{-1})
k_c		Attenuation coefficient for chlorophyll (m^{-1})
k_i	[0.035, 0.057, 0.035]	Algal specific light attenuation coefficient (m^2 (mg chl)$^{-1}$)
CDM		Attenuation of blue light by CDOM as a function of salinity (m^{-1})
X_1		Nitrification rate - water column (umoles N Kg^{-1} s^{-1})
X_{ls}		Nitrification rate - sediment (umoles N Kg^{-1} s^{-1})
β_s	0.01	Dissolution rate of particulate silicate in sediment (d^{-1})
λ_i	0.05	Degradation rate of particulate organic carbon in sediment (d^{-1})
K_b	2.0×10^{-10} $e^{0.092Tb}$	Bioturbation coefficient in relation to bottom temperature T_b (m^2 s^{-1})
K_m	3.5×10^{-10}	Porewater diffusion coefficient (m^2 s^{-1})
chl	[0.50, 0.05, 1.00]	Chlorophyll content ($\times 10^{-5}$ ug chl $cell^{-1}$)
C/Chl	[50, 100, 30]	Particulate organic carbon/chlorophyll ratio (ug/ug)

slope to both the 30-m and 45-m isobaths. However, given a maximum diatom growth rate of 1.1 d^{-1} at 20°C and a half-saturation constant of 1.05 umol NO_3 kg^{-1} (Table 2), these WFS diatoms should have accumulated 10 ug chl L^{-1} within a few days, not over a few weeks.

[22] During this period, SeaWiFS imagery indicated that a major southwestward export of surface color had occurred, progressing from coastal waters in the Big Bend region to the Dry Tortugas [*Jolliff et al.*, 2003] and following the trajectory of previous surface drifters [*Yang et al.*, 1999]. As in May, the early June 1998 extracted chlorophyll was fivefold less than the satellite estimate, where ground truth data were available. These results suggested an export of mainly CDOM,- perhaps 80% of the color signal,- within the surface Ekman layer. After this time, surface stratified waters (Figure 4a) had <0.1 umol NO_3 kg^{-1}(Figure 4b) and a mean del^{15}PON value of ~+8.0‰ on 7 July 1998 (Table 1), i.e., the expected final isotopic signature of nitrate-stripped source waters.

3.1.2. Model Results

[23] Details of the computed flow fields are given in this volume [*Weisberg and He*, 2003]; their consequences are presented here. As in the real world (Figure 3a), when strong coastal upwelling by the Loop Current and large CDOM loading prevailed in the first case, the 1 umol NO_3 kg^{-1} isopleth of the near-bottom nitrate field penetrated to the ~20-m isobath in the Big Bend region by 19 May (Figure 7a). On the 30-m isobath off Sarasota, 1.4 umol NO_3 kg^{-1} was computed there at 1 m above the bottom (Table 3), similar to that inferred from sparse observations (Figure 4b). With neither the Loop Current nor the CDOM-induced light limitation, however, the 1 umol NO_3 kg^{-1} isopleth of the second case instead penetrated to only the ~35-m isobath in the Big Bend region by 19 May (Figure 8a), while just ~0.1 umol NO_3 kg^{-1} was then simulated off Sarasota (Table 3).

[24] Later on 8 June, the first case of strong flows, CDOM light limitation, and consequently smaller primary production and algal biomass (Figure 7d) yielded near-bottom recycled nitrogen stocks of >1 umol NH_4 kg^{-1} along the inner shelf between Apalachicola and Tampa Bays (Figure 7b), similar to the NEGOM observations during July–August 1998 (Figure 6b). On the Sarasota line, 0.8 umol NH_4 kg^{-1} had formed at the 30-m isobath in the first

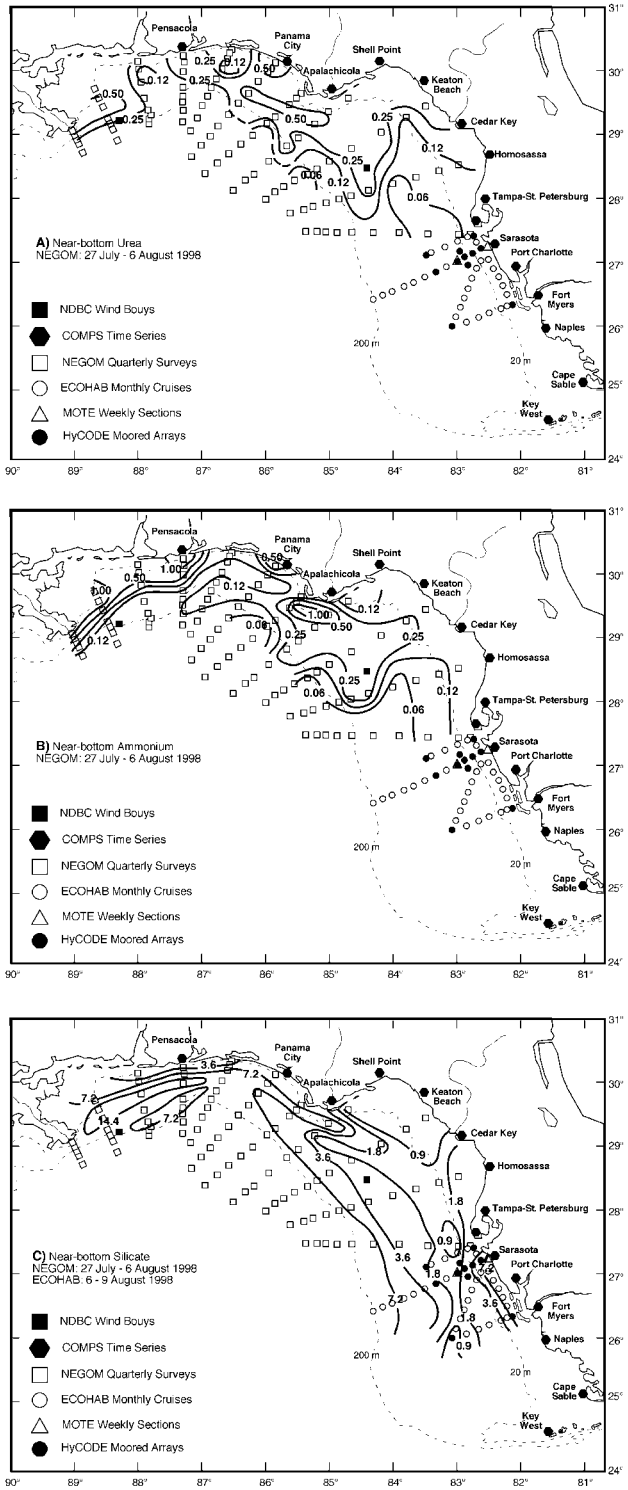

Figure 6. A summer composite of the near-bottom fields (μmol kg^{-1}) of (a) urea, (b) ammonium, and (c) silica found by ECOHAB/NEGOM surveys of the West Florida Shelf during 25 July to 9 August 1998.

case by then (Table 3). In contrast, the near-bottom pool of >1 umol NH_4 kg^{-1} of the second case was simulated much farther offshore on 8 June, along the ~75-m isobath of the outer shelf (Figure 8b). Inside the 20-m isobath of the Panhandle, maximal near-bottom ammonium stocks (denoted by "M") on June 8 were 2.9 umol NH_4 kg^{-1} in the first case (Figure 7b), compared to 8.0 umol NH_4 kg^{-1} in the second (Figure 8b).

[25] The near-bottom silicate fields of the two cases on 8 June (Figures 7c and 8c) exhibited the same tongue-like feature of upwelled water, moving southeast along the 40-m isobath. In both cases, the microflagellates of the Big Bend region were then the dominant phytoplankton group of ~1.2–1.6 ug chl L^{-1}, compared to 0.2–0.3 ug chl L^{-1} of diatoms and $\ll$0.1 ug chl L^{-1} of *K. brevis*. Thus the unutilized 1.2–2.4 umol SiO_4 kg^{-1} simulated off Sarasota on June 8 did not induce Si limitation of diatoms in either case (Table 3), while their maximal stocks were the same (14.2–14.4 umol SiO_4 kg^{-1}) on the Alabama shelf (Figures 7c and 8c).

[26] The CDOM limitation of case 1 allowed only 1.9 watts m^{-2} of PAR to reach bottom on June 8 off Sarasota, compared to a penetration of 13.9 watts m^{-2} in the second scenario (Table 3). Consequently, the diatoms were light-limited over 38% of the water column in case 1, but not at all in case 2. Nitrogen limitation was more severe in case 2, however, as a result of upstream depletion, yielding smaller amounts of total phytoplankton biomass. At this point, microflagellates were the winners in both cases of the models off Sarasota (Figures 7e–7g and 8e–8g), with most of their primary production consumed by protozoans (Table 3).

[27] Much larger differences of phytoplankton biomass between the two cases were simulated on the northern WFS, where 4.5 ug chl L^{-1} were predicted off Apalachicola in the second (Figure 8d), compared to 1.6 ug chl L^{-1} in the first (Figure 7d). Here, diatoms and microflagellates were codominants in the CDOM-free case. How realistic are such phytoplankton accumulations in the absence of terrestrial CDOM? May they instead represent other microflora, sea grass, and macroalgae, not considered as state variables of this model? We shall find that these nearshore maxima increased to 19.2–21.1 ug chl L^{-1} by 7 August in both cases (Figures 9d and 10d), in case 1, because of greater onshore flows in the bottom Ekman layer, and in case 2, because of no light attenuation by CDOM.

3.2. Summer Slow Down: Doldrums, Downwelling, and Diazotrophs

3.2.1. Observations

[28] The anomalous west winds in the northern Gulf of Mexico continued during June–July 1998 (Figure 2a), such that the August 1998 sea surface temperatures near the Panhandle coast remained ~2°C colder than on the Alabama shelf [*Muller-Karger*, 2000]. The NEGOM/ECOHAB/HyCODE nutrient data also indicated that deeper source waters now impacted the outer WFS between Pensacola and Tampa, with a mean bottom water stock of 21.1 umol NO_3 kg^{-1} in August at the 200-m isobath (Figure 3b), compared to 14.4 umol NO_3 kg^{-1} in May (Figure 3a). However, the local upwelling favorable winds were weaker, because summer south winds now prevailed off Sarasota, as part of the usual seasonal transition [*Yang and Weisberg*, 1999].

[29] During the last half of July and the first week of August 1998, a weak downwelling circulation was found at the ADCP arrays (Figure 1) under local south winds, such

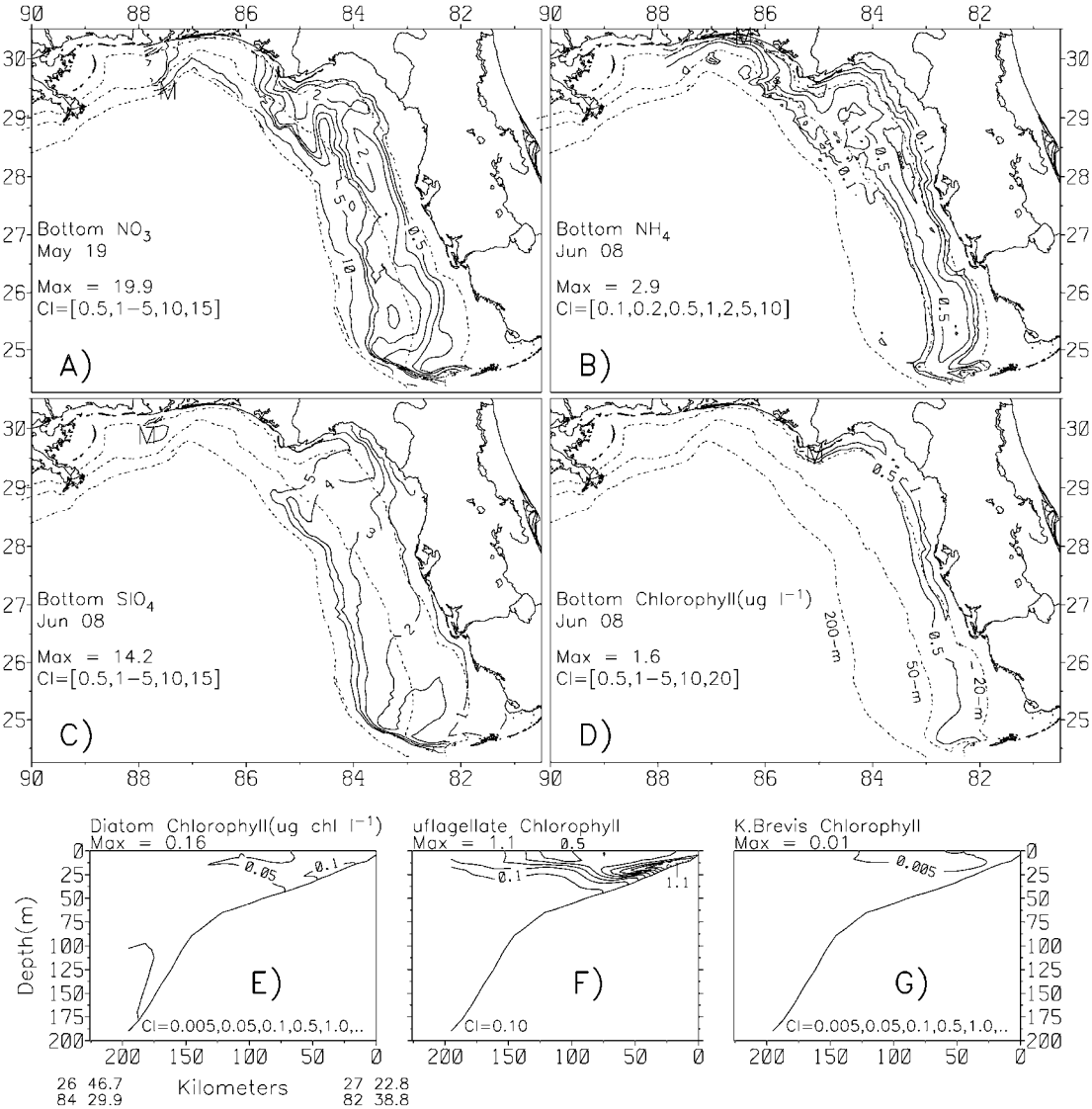

Figure 7. The computed (a) near-bottom 19 May nitrate field in relation to both the near-bottom 8 June fields of (b) ammonium, (c) silicate, and (d) chlorophyll and the Sarasota June sections of (e) diatom, (f) microflagellate, and (g) *K. brevis* chlorophyll stocks under CDOM and Loop Current forcings. The 20, 50, and 200-m isobaths are delineated by dashed lines, and the location of the maximum value is denoted by the symbol M.

that near-bottom stocks continued to be <0.1 umol NO_3 kg^{-1} at the 30-m isobath (Figure 4b). Yet, the surface phytoplankton populations had the lowest $del^{15}PON$ value of +2.7‰ on 7 August 1998 (Table 1), despite stocks of $\leq$0.01 umol NO_3 kg^{-1}over the upper water column. Although the supply of nitrate from the major spring intrusion of slope waters had now been depleted, uptake of the enriched ^{15}N nitrate left behind in the water column was evidently not the major new nitrogen signal, implying that nitrogen fixation was instead the source of PON. Indeed, surface colonies of WFS *Trichodesmium* had $del^{15}N$ values of -0.6 to -0.8‰ during September/October 2000 (Table 1).

3.2.2. Model Results

[30] The MODIS CDOM algorithm indicated that most of the dissolved color signal was flushed from the WFS by the end of June in the real world [*Jolliff et al.*, 2003]. Thus our case 1 results of the near-bottom nitrate on 7 August (Figure 9a) reflected too much light limitation by CDOM, with too little nitrate utilization by the phytoplankton (Figure 9d). The 1 umol NO_3 kg^{-1} isopleth of near-bottom nitrate remained at the ~20-m isobath of the Big Bend region in case 1 (Figure 9a). In contrast, it was found along the ~65-m isobath (Figure 3b) and simulated there in case 2 (Figure 10a). Consequently, <0.1 umol NO_3 kg^{-1} was left unutilized off Sarasota on 7 August in case 2, compared to 5.5 umol NO_3 kg^{-1} predicted by case 1 (Table 3). Nitrate limitation then prevailed over 70% of the simulated CDOM-free, well-lit water column, suggesting that a much larger $del^{15}PON$ value than +2.7‰ should have been measured, if nitrate were the only source of new nitrogen.

Table 3. Simulated Plankton Dynamics of Light Penetration, Primary Production, Nutrient Utilization, Growth Limitation, Phytoplankton Dominance, CO_2 Evasion, and Grazing Losses at the 30-m Isobath of the Sarasota Line During 1998 Under Both (A) CDOM/Loop Current Forcings and (B) Their Absence

	May 19	June 8	July 8	Aug. 7	Sep. 21	Oct. 11	Nov. 10	Dec. 15
				Near-Bottom Isolume, I ($W\ m^{-2}$)				
A	3.55	1.94	0.26	0.07	0.01	0.02	0.02	0.00
B	14.11	13.91	11.13	10.64	11.97	12.27	3.65	2.02
				Net Photosynthesis ($g\ C\ m^{-2}d^{-1}$)				
A	0.28	0.28	0.25	0.22	0.05	0.02	0.26	0.14
B	0.17	0.13	0.13	0.13	0.05	0.05	0.39	0.17
				Near-bottom Nitrate Stock[a] ($umol\ N\ kg^{-1}$)				
A	1.35	1.25	2.81	5.53	0.15	0.31	1.95	2.03
B	0.04	0.03	0.03	0.02	0.01	0.01	0.09	0.02
				Near-Bottom Ammonium Stock[a] ($umol\ N\ kg^{-1}$)				
A	0.14	0.83	0.48	0.90	0.11	0.20	0.18	0.03
B	0.06	0.07	0.08	0.09	0.01	0.02	0.17	0.04
				Near-Bottom Silicate Stock[a] ($umol\ Si\ kg^{-1}$)				
A	2.15	2.39	2.77	4.16	2.63	2.78	3.14	3.07
B	1.49	1.20	1.24	1.07	1.33	1.88	2.10	2.13
				Growth Limitation (% I, % NO_3 + NH_4, % Si Over the Water Column)				
Diatom								
A	40,60,0	38,62,0	51,49,0	39,61,0	8,92,0	11,99,0	19,81,0	11,89,0
B	2,98,0	0,100,0	1,99,0	1,99,0	0,100,0	0,100,0	5,95,0	1,99,0
Microflagellate								
A	49,51,...	47,53,...	58,42,...	47,53,...	21,79,...	21,79,...	40,60,...	32,68,...
B	7,93,...	6,94,...	7,93,...	7,93,...	1,99,0	2,98,0	35,65,...	24,76,...
Karenia brevis								
A	49,51,...	53,47,...	66,34,...	59,41,...	28,72,...	22,78,...	45,55,...	37,63,...
B	26,74,...	23,77,...	19,81,...	18,82,...	15,85,...	16,84,...	21,79,...	17,83,...
				Maximum Diatom Chlorophyll Stock[a] *at Depth* (*m*)				
A	0.06(22)	0.12(22)	0.25(13)	0.80(13)	0.62(30)	0.66(15)	0.64(2)	0.47(3)
B	0.04(30)	0.05(29)	0.09(30)	0.21(30)	0.11(30)	0.13(30)	0.99(30)	0.58(30)
				Maximum Mflagellate Chlorophyll Stock[a] *at Depth* (*m*)				
A	0.66(17)	0.86(20)	0.78(10)	0.69(8)	0.36(0)	0.20(8)	0.34(0)	0.15(0)
B	0.66(29)	0.68(30)	0.64(30)	0.76(30)	0.25(8)	0.26(30)	0.75(30)	0.43(0)
				Maximum K. brevis Chlorophyll Stock[b] *at Depth* (*m*)				
A	0.00	0.00	0.06(6)	1.97(3)	11.70(0)	11.00(0)	4.52(0)	8.46(0)
B	0.00	0.00	0.02(27)	0.05(27)	0.03(29)	0.08(30)	0.14(0)	1.08(0)
				CO_2 Invasion (+ $g\ C\ m^{-2}d^{-1}$)				
A	−0.05	−0.09	−0.09	−0.07	−0.03	−0.01	+0.03	+0.06
B	−0.12	−0.14	−0.13	−0.10	−0.08	−0.06	0.00	+0.01
				Copepod Grazing ($g\ C\ m^{-2}d^{-1}$)				
A	0.00	0.00	0.02	0.04	0.00	0.00	0.04	0.00
B	0.00	0.00	0.00	0.00	0.00	0.00	0.04	0.02
				Protozoan Grazing ($g\ C\ m^{-2}d^{-1}$)				
A	0.14	0.25	0.21	0.14	0.08	0.03	0.07	0.01
B	0.14	0.13	0.13	0.12	0.05	0.05	0.29	0.14

[a]Average over the lower 1 m of the water column, since in situ sampling ignores POM's Ekman layer.
[b]Vertical migration of *Karenia brevis* can lead to subsurface aggregations.

[31] No silica limitation of diatoms pertained in case 2 at the 30-m isobath of the Sarasota line (Table 3), but farther offshore a minimum of <0.9 umol SiO_4 kg^{-1} was computed on 7 August (Figure 10c), again similar to that measured (Figure 6c) and not simulated in case 1 (Figure 9c). During all of August in case 2, diatoms were silica-limited along the 40–50 m isobaths from the Big Bend region to the Sarasota section. Ammonium was more effectively recycled than silicon in case 2, with a maximum accumulation of >2 umol NH_4 kg^{-1} in outer shelf regions (Figure 10b), where near-bottom silicate stocks were minimal.

[32] The total phytoplankton biomasses of 1.0–3.4 ug chl L^{-1} on the Sarasota line in both cases on 7 August (Table 3) were similar to those observed (Figure 4c), but the midshelf maxima of diatoms in case 2 was a more realistic depiction of cross-shelf observations. The complete floral composition and vertical distributions of the two scenarios

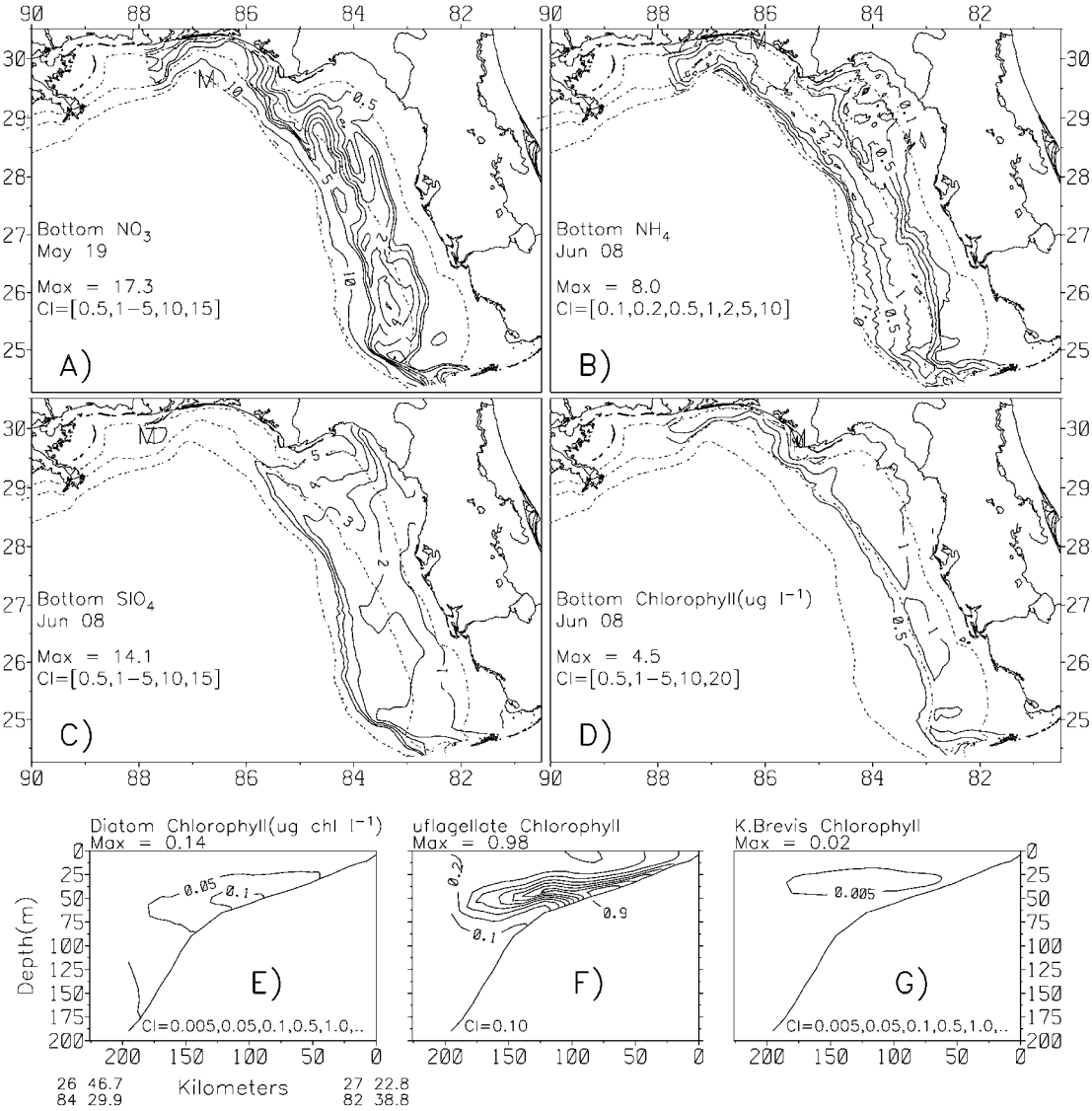

Figure 8. The computed (a) near-bottom 19 May nitrate field in relation to both the near-bottom 8 June fields of (b) ammonium, (c) silicate, and (d) chlorophyll and the Sarasota June sections of (e) diatom, (f) microflagellate, and (g) *K. brevis* chlorophyll stocks with neither CDOM nor Loop Current forcings.

were also very different (Figures 9e–9g and 10e–10g). A red tide of 2.0–2.7 ug chl L^{-1} of *K. brevis* was predicted at depth of 3 m in case 1 (Figure 9g and Table 3), but not observed during ECOHAB/MOTE surveys. Only their background populations of 0.05 ug chl L^{-1} were simulated in case 2 (Figure 10g) and found in August and September, such that their small bloom did not begin in the real world until November.

3.3. Fall Fertilization: Local Upwelling and Phytoplankton Blooms

3.3.1. Observations

[33] The Panhandle winds were no longer from the west during November 1998 (Figure 2a). Without upwelling in De Soto Canyon, the mean bottom water nitrate at the 200-m isobath had relaxed to 16.9 umol NO_3 kg^{-1} in November 1998 (Figure 3c), compared to 21.1 umol NO_3 kg^{-1} in August (Figure 3b), and 14.4 umol NO_3 kg^{-1} in May (Figure 3a). Once this upstream supply was eliminated, decreasing amounts of slope water nutrients remained on the outer WFS to fuel diatom growth during successive fall upwelling events (Figure 4).

[34] For example, after initial destratification of the water column (Figure 4a), strong upwelling winds during 7–14 October 1998 provided 3.2 umol NO_3 kg^{-1} to the 30-m isobath by 11 October (Figure 4b), compared to 0.7 umol NO_3 kg^{-1} on 6 October. Here, the phytoplankton responded with another near-bottom biomass accumulation of 2.2 ug chl L^{-1} (Figure 4c). Their surface $del^{15}PON$ value was now a mean of +3.6‰ (Table 1), reflecting both the expected fractionation of recently supplied nitrate and vertical mixing of phytoplankton throughout the upper water column.

[35] In contrast, after more upwelling-favorable winds during 4–7 November 1998, only 1.1 umol NO_3 kg^{-1}

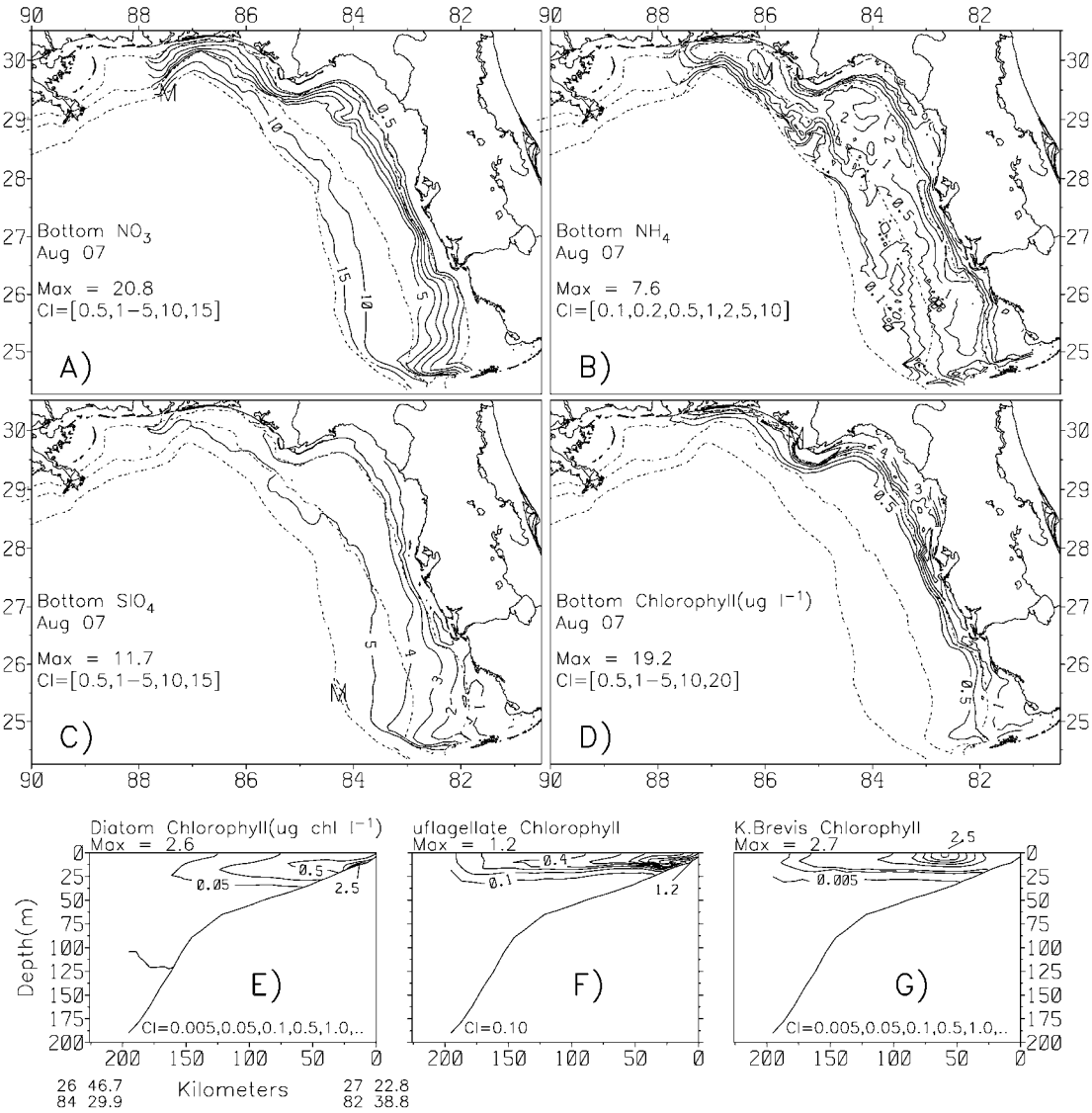

Figure 9. The computed near-bottom fields of (a) nitrate, (b) ammonium, (c) silicate, and (d) chlorophyll in relation to the Sarasota sections of (e) diatom, (f) microflagellate, and (g) *K. brevis* chlorophyll stocks on 7 August under CDOM and Loop Current forcings.

and 0.7 umol SiO_4 kg^{-1} penetrated to the 30-m isobath on 10 November (Figure 4b), producing the same near-bottom phytoplankton biomass of 2.5 ug chl L^{-1} (Figure 4c). Moreover, the mean surface $del^{15}PON$ value was then +6.80‰ (Table 1), reflecting the enriched ^{15}N left behind in the smaller pool of slope water nitrate.

3.3.2. Model Results

[36] During the November upwelling event, the stronger near-bottom flows in case 1 more faithfully replicated the observed nitrate field (Figure 3c) on 10 November (Figure 11a), compared to case 2 with no Loop Current (Figure 12a). Despite the greater near-bottom simulated stock of ~2.0 umol NO_3 kg^{-1} off Sarasota in case 1, 81% of the diatom populations were still nitrate-limited (Table 3), consistent with the $del^{15}PON$ measurements (Table 1). Yet, the negative impact of CDOM light limitation in the models was more important in replicating the phytoplankton observations than the positive effect of greater nutrient supply.

[37] The near-bottom phytoplankton community of 1.7 ug chl L^{-1} on 10 November in case 2 (Figures 12e–12g) instead matched the data (Figure 4c), whereas the near-surface 7.4 ug chl L^{-1} of case 1 (Figures 11e–11g) did not. Furthermore, the floral composition of case 1 continued to be dominated by red tides, that were not found in the real world. A massive surface bloom of >5 ug chl L^{-1} of *K. brevis* was incorrectly predicted from the coast out to the 50-m isobath (Figure 11g). Case 2 instead produced 0.1 ug chl L^{-1} of *K. brevis* near the coast (Figure 12g) as found on the November MOTE/ECOHAB surveys. Attenuation of light by the large red tide in case 1, only 0.02 watts m^{-2} penetrated to the 30-m isobath (Table 3), allowed no development of the near-bottom diatom populations (Figure 11e), which were

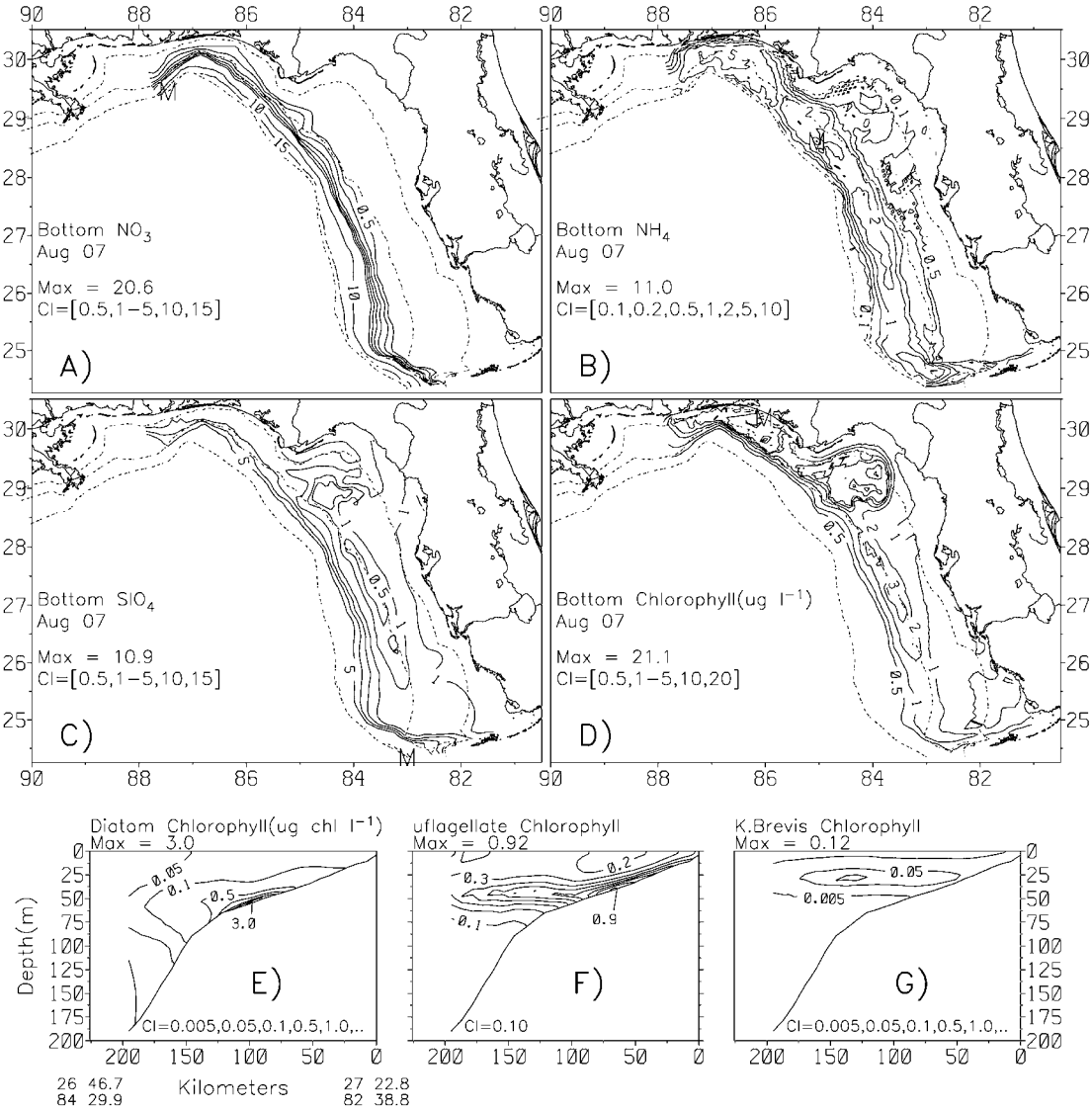

Figure 10. The computed near-bottom fields of (a) nitrate, (b) ammonium, (c) silicate, and (d) chlorophyll in relation to the Sarasota sections of (e) diatom, (f) microflagellate, and (g) *K. brevis* chlorophyll stocks on 7 August with neither CDOM nor Loop Current forcings.

simulated in case 2 (Figure 12e) and also observed (Figure 4c).

3.4. Winter Windows: Yuletide or Red Tide?

3.4.1. Observations

[38] Despite upwelling favorable winds, no additional influxes of nitrate were found at the 30-m isobath (Figure 4b) after the 2 and 21 December events. One might expect the surface phytoplankton community to reflect these shortages of new nitrogen, with perhaps a similar value to the mean del^{15}PON of +8.0‰ found in the July, September, and November populations (Table 1). Instead, the December del^{15}PON mean value was +5.8‰, suggesting possible bacterial reprocessing of the residues of pelagic and/or benthic nitrogen fixation [*Walsh and Steidinger*, 2001].

[39] Samples dominated by *K. brevis* had positive del^{15}PON values of 3.6 to 5.1‰ in October 2000, 4.4‰ in October 1999, and 4.9‰ in December 1998 (Table 1). Values of +3 to 5‰ were found for the 2001 red tide as well. Organic nitrogen released from *Trichodesmium* spp., seagrasses, mangroves [*O'Donohue et al.*, 1998; *Corbett et al.*, 1999], and even agricultural leachates [*Fryer and Aly*, 1974; *Kreitler*, 1979] may all supply an isotopic nitrogen-fixation signal for *K. brevis*, such that specific DON supplies have yet to be identified [*Heil et al.*, 2002; *Lester et al.*, 2002]. However, in this analysis, we can at least address the null hypothesis that the amount of slope water nutrients would have been insufficient to support a red tide of ~5 ug chl L^{-1} in December 1998 on the WFS.

3.4.2. Model Results

[40] Without diatom removal of near-bottom nitrate in case1 during November, the failure of this model scenario became worse in December. By 15 December, case 1 incorrectly predicted 2.0 umol NO_3 kg^{-1} along the inner shelf (Figure 13a), as far south as Sarasota (Table 3).

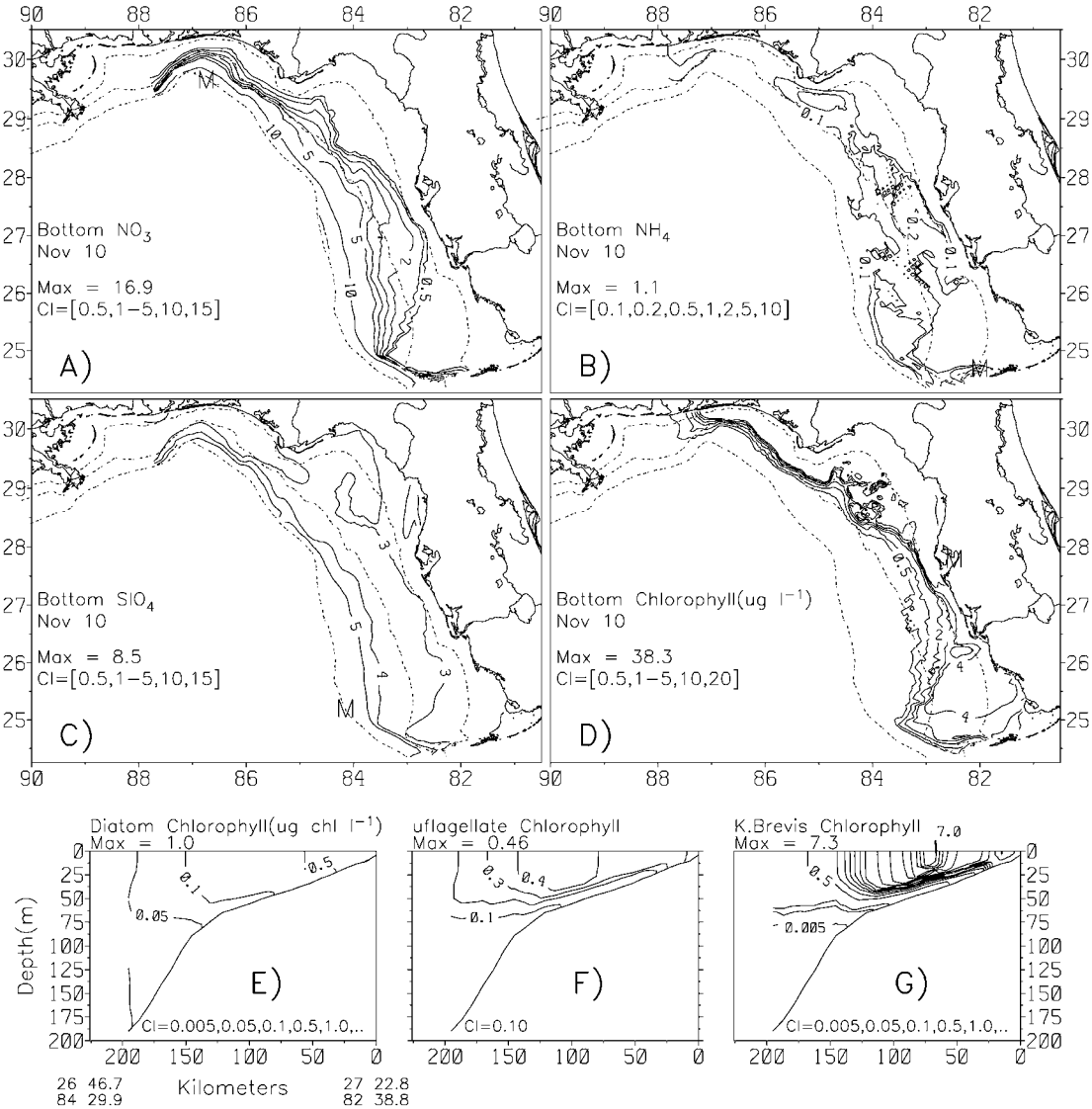

Figure 11. The computed near-bottom fields of (a) nitrate, (b) ammonium, (c) silicate, and (d) chlorophyll in relation to the Sarasota sections of (e) diatom, (f) microflagellate, and (g) *K. brevis* chlorophyll stocks on 10 November under CDOM and Loop Current forcings.

Less than 0.1 umol NO_3 kg^{-1} were then observed (Figure 4b) and simulated there in case 2 (Figure 14a). In terms of diatom biomass, light limitation of case 1 (Figure 13e) and nitrate limitation of case 2 (Figure 14e) both yielded pigment stocks of ~0.5 ug chl L^{-1} as observed (Figure 4c).

[41] The case 1 red tide of >15.0 ug chl L^{-1} now extended out to the shelf-break during 15 December (Figure 13g), however, and was not seen by either SeaWiFS, or ECOHAB observers. Yet, case 2 predicted a red tide of only 0.5 ug chl L^{-1} near the coast (Figure 14g), where at least 5.0 ug chl L^{-1} were found between Tampa Bay and Fort Myers. In the real world, other supplies of both aeolian and estuarine nutrients are required to form a larger red tide than that now simulated in case 2 of the coupled models. Furthermore, an estuarine source of CDOM at the local scale of a convergence front is required to allow shade-adapted *K. brevis* to both out compete diatoms and microflagellates, and aggregate over a region of smaller spatial extent, not the shelf-wide feature of the case 1 red tide.

4. Discussion

[42] In response to upwelled intrusions of nitrate-rich slope water onto the WFS of our coupled models, diatoms won over both microflagellates and toxic dinoflagellates, if light limitation by CDOM was only applied over May–June and then deleted during July–December. Selective grazing stress and at times Si limitation completed a numerical description of how not to make a red tide! Given the models' reasonable fidelity with the results of 18 cruises in 1998 (Figure 1), what are the implications for carbon cycling, its transfer to higher trophic levels, and its partition among phytoplankton competitors during this and other years?

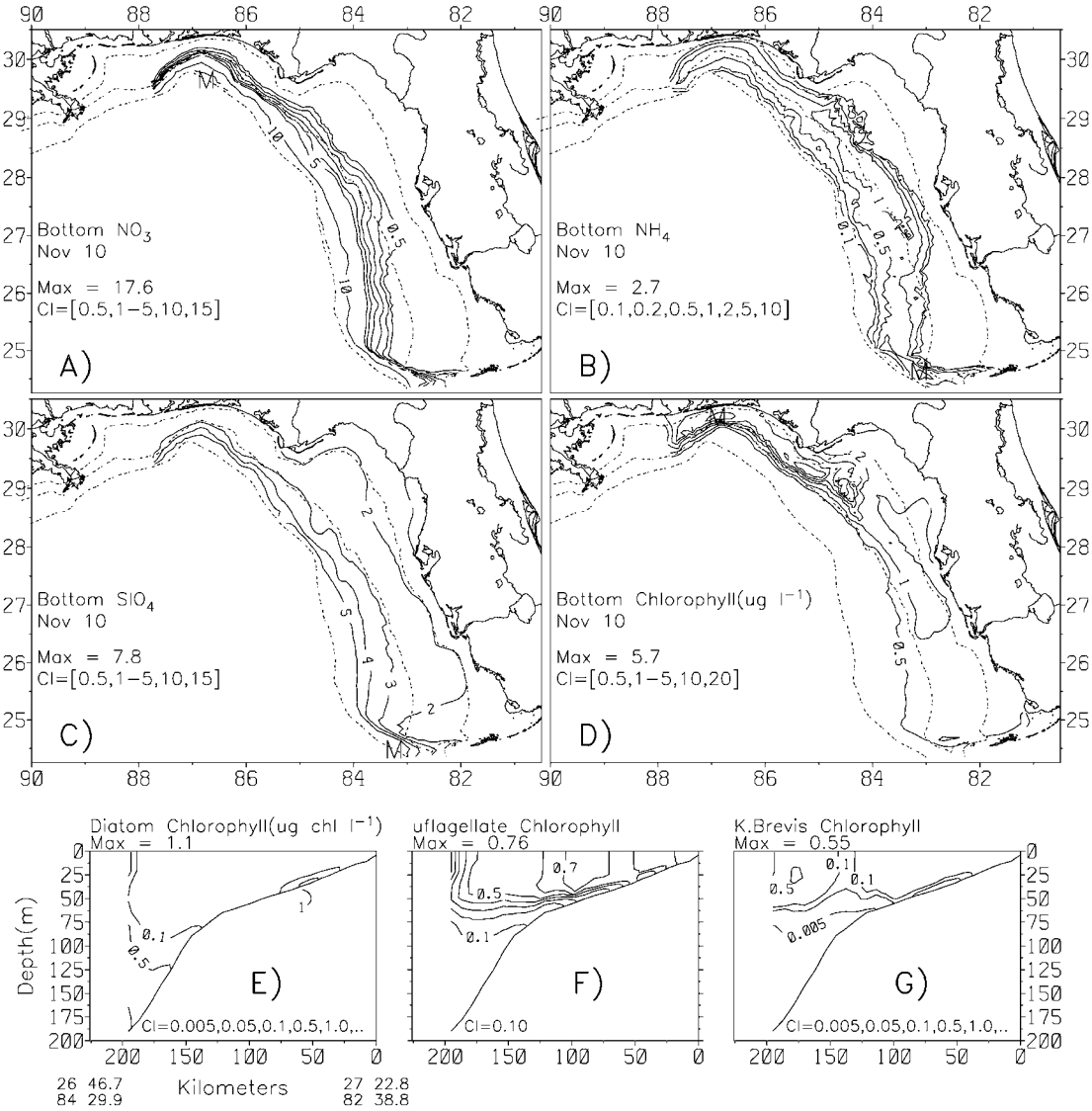

Figure 12. The computed near-bottom fields of (a) nitrate, (b) ammonium, (c) silicate, and (d) chlorophyll in relation to the Sarasota sections of (e) diatom, (f) microflagellate, and (g) *K. brevis* chlorophyll stocks on 10 November with neither CDOM nor Loop Current forcings.

[43] Within low-salinity waters of 27.9–31.2 psu on the WFS, measured CDOM absorption at 412 nm and DOC stocks [*Del Castillo et al.*, 2000], together with a spectral slope of 0.020 nm^{-1} and a specific CDOC absorption of 0.151 mg^{-1} CDOC m^{-1} [*Walsh and Dieterle*, 1994], suggested that CDOC stocks were 52–100% of the DOC concentrations at 443 nm during March, similar to prior estimates in April [*Harvey et al.*, 1983; *Carder et al.*, 1989]. In contrast, at a salinity of 36.2 psu, CDOC was only ~10% of the DOC, such that the amounts of CDOC ranged from 202 umol L^{-1} on the inner WFS to 12 umol L^{-1} in the outer regions. The cross-shelf range of total DOC range was smaller, from 272 to 126 umol DOC L^{-1}.

[44] Photodegradation studies of riverine CDOM, including Suwannee and Everglades sources, suggest a minimal photolysis rate of ~3.0 umol CDOC L^{-1} d^{-1} over a 12-hour photoperiod [*Keiber et al.*, 1990]. At such a rate, ultraviolet radiation within the upper 5 m of the WFS might take ~2 months to convert 190 umol CDOC L^{-1} of macromolelcular CDOM to small molecules of colorless DOM, and thence to DIC at perhaps a slower rate [*Andrews et al.*, 2000]. Furthermore, we have found that the sediment microfloral biomass on the 10–60 m isobaths of the WFS is usually twofold to fourfold larger than those of phytoplankton in the overlying water column. Thus severe CDOM attenuation of light must be the exception on most of the WFS, not the norm.

[45] A one-dimensional model of both phytoplankton and sediment microflora [*Darrow et al.*, 2003] was able to replicate the demise of the April 1996 diatom bloom at the 27-m isobath of the Big Bend region [*Hitchock et al.*, 2000]. It also matched the subsequent seasonal increase of sediment pigments here, if CDOM absorption at 443 nm was <0.15 m^{-1}. Part of the near-bottom pigment stocks of

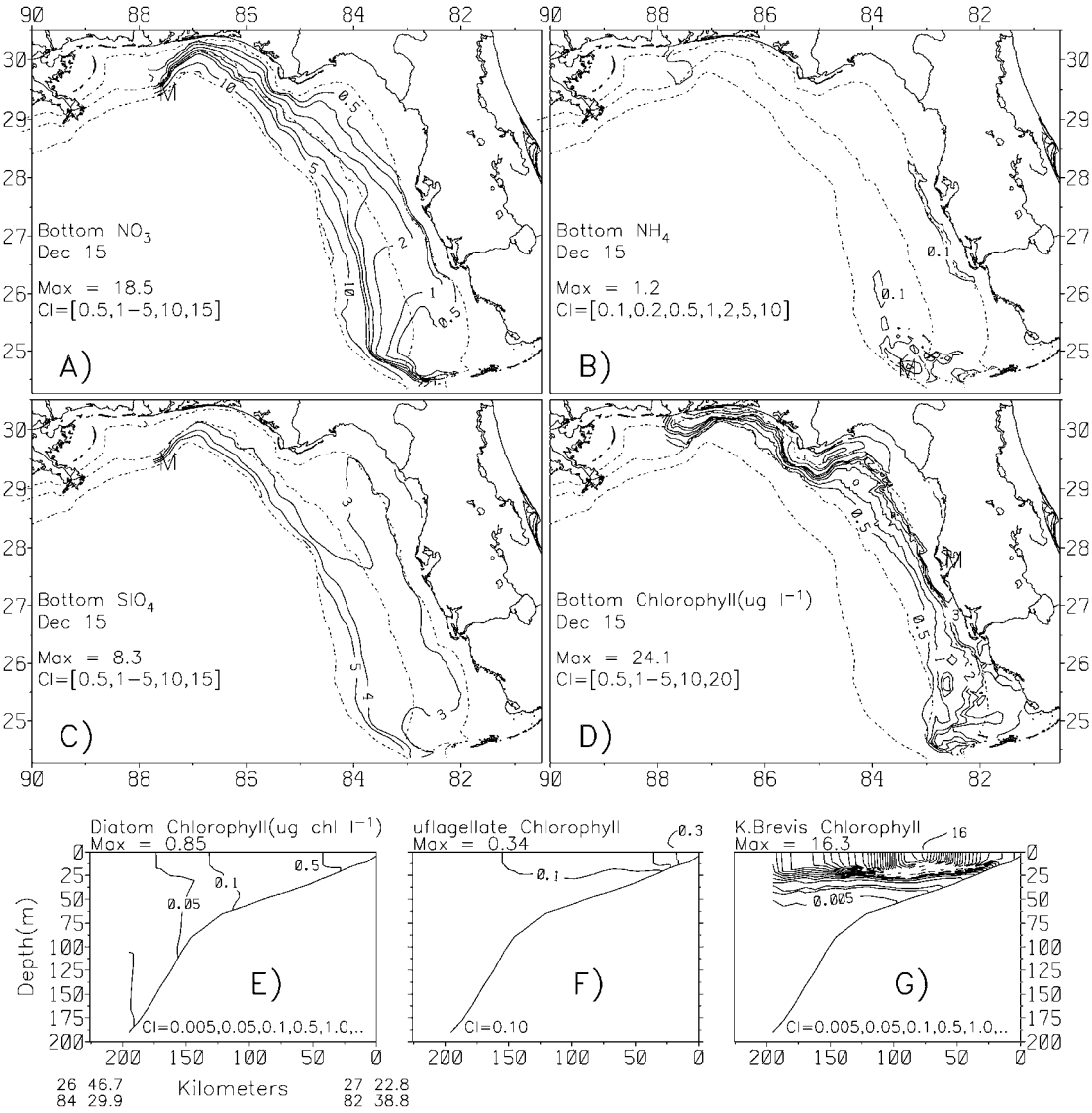

Figure 13. The computed near-bottom fields of (a) nitrate, (b) ammonium, (c) silicate, and (d) chlorophyll in relation to the Sarasota sections of (e) diatom, (f) microflagellate, and (g) *K. brevis* chlorophyll stocks on 15 December under CDOM and Loop Current forcings.

19.2–21.1 ug chl L^{-1} on 7 August in both cases of the present 3-D model (Figures 9d and 10d) may thus represent ignored sediment microflora. *Cladophora* spp. are invasive green macroalgae [*LaPointe and O'Connell*, 1989], known colloquially as "June grass" along Panama City in the Panhandle. They washed ashore there during June 1998. With light saturation intensities tenfold greater than those of *K. brevis*, however, the macroalage are probably confined to shallow waters, like the Big Bend seagrass beds of <4 m depth [*Iverson and Bittaker*, 1986].

[46] If estuarine supplies of CDOM are usually restricted to depths of <10 m as a result of photolysis, allowing large amounts of benthic plants, then slope water intrusions may generally experience light regimes typified by the case 2 results. During August 1998, this simulated total primary production was ~1.8 g C m^{-2} d^{-1} along the 40-m isobath in the northern part of the WFS, with an accumulated biomass of >10.0 ug chl L^{-1} on the Florida Middle Ground (FMG) at ~28°10′–28°45′N, 84°–84°25′W (Figure 10d). Similar ^{14}C estimates of 1–3 g C m^{-2} d^{-1} were made here by us during August 1992–1993, compared to <0.5 g C m^{-2} d^{-1} found and simulated farther south. In terms of carbon sequestration, this 3-D model, like previous 1-D ones [*Walsh and Dieterle*, 1994; *Darrow et al.*, 2003] mainly evaded CO_2 from the WFS (Table 3), although there were episodes of invasion, particularly in the Big Bend region as found in 1996 [*Wanninkhof et al.*, 1997].

[47] Diatom losses of ~90% of their daily carbon fixation to herbivores on the FMG in August of case 2 supported earlier impressions of a short, diatom-based food web in this region of the shelf. Here organic carbon content of surficial sediments is ten-fold those of the surrounding seabeds [*Walsh et al.*, 1989], implying fallout of larger cells, i.e., diatoms [*Gilbes et al.*, 2002]. Within Apalachicola Bay and

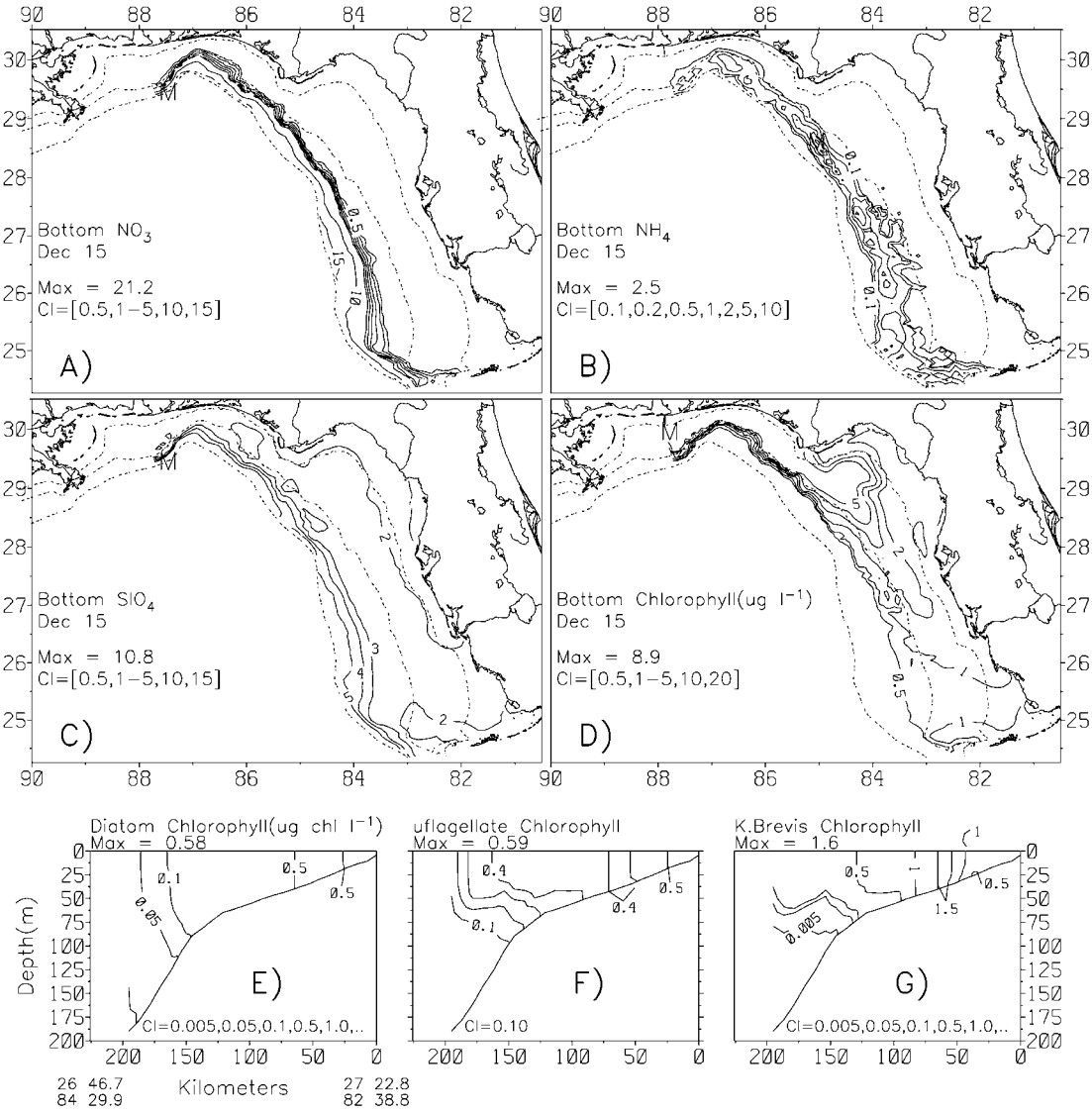

Figure 14. The computed near-bottom fields of (a) nitrate, (b) ammonium, (c) silicate, and (d) chlorophyll in relation to the Sarasota sections of (e) diatom, (f) microflagellate, and (g) *K. brevis* chlorophyll stocks on 15 December with neither CDOM nor Loop Current forcings.

Alligator Harbor, spring diatom blooms of 5–7 ug chl L^{-1} and productivities of ~1.7 g C m^{-2} d^{-1} have been reported in March–April [*Marshal*, 1956; *Livingston*, 1984]. The seasonal harvest of these neritic species, i.e., *Chaetoceros* and *Rhizosolenia* [*Curl*, 1959; *Hopkins*, 1966], was thought to fuel copepod and sardine populations over the northern half of the shelf [*Khromov*, 1969; *Austin and Jones*, 1974]. Episodic diatom blooms, driven by summer intrusions of slope water, may do the same.

[48] In contrast, farther south off Sarasota the simulated copepods of case 2 only removed 0.04 g C m^{-2} d^{-1}, about 25% of the diatom production, by November. The protozoans instead cropped most of the microflagellate yield (Table 3). Recall that little grazing loss was imposed on the small red tide of case 2. During September 1998, the estimated ingestion demands of the observed zooplankton community yielded the same crustacean grazing stress off Sarasota [*Sutton et al.*, 2001]. At the 30-m isobath, they estimated that all of the zooplankton community may have removed 0.08 ug chl L^{-1} d^{-1}, or 0.12 g C m^{-2} d^{-1} with diatom C/chl ratio of 50 (Table 2); that is, the copepods ate 34% compared to 66% by the larvaceans.

[49] Although copepods generally shun *K. brevis*, those zooplankton grown on diatom-rich intrusions of slope water, as in 1998, may switch to toxic dinoflagellates, once prey stocks of diatoms are negligible. Top-down controls may thus possibly prevent formation of large red tides during years of strong upwelling, when supplies of Saharan dust, nitrogen fixers, and estuarine phosphorus may otherwise be sufficient [*Walsh and Steidinger*, 2001]. The role of local light shading by CDOM may be equally important as grazing, however, as demonstrated by the enormous red tide of case 1, in allowing surface populations of dark-adapted *K. brevis* to accumulate [*Walsh et al.*, 2002].

[50] Each year, *K. brevis* may need the CDOM of case 1 over a smaller coastal region of the WFS to avoid photo-

inhibition [*Millie et al.*, 1995]. During another red tide of 32 ug chl L^{-1} in October 1983, for example, a CDOM absorption of 0.30 m^{-1} still contributed 25% of the total color signal [*Carder and Steward*, 1985]. Furthermore, *Trichodesmium* is a source of CDOM [*Jones et al.*, 1986], providing both sun screen and nutrients to *K. brevis*. Finally, the small del^{15}PON tag of the December phytoplankton community (Table 1) reflected nitrogen fixation, and we could not replicate that bloom in case 2 without a N_2 source of new nitrogen.

[51] The local upwelling (Figure 15), focused by the bathymetry [*Weisberg et al.*, 2000], may thus promote aggregation of and recycled nitrogen transfer between diazotrophs and *K. brevis* within nitrate-poor waters at salinity fronts of estuarine phosphorus supplies [*Walsh and Steidinger*, 2001; *Lenes et al.*, 2001; *Walsh et al.*, 2002]. Once a diatom, microflagellate, or dinoflagellate population is upwelled into surface waters of the coastal zone (Figure 15), all of these factors will come into play. Furthermore, the same local nearshore waters of the WFS that provide salinity fronts for aggregating diazotrophs and *K. brevis*, terrestrial P supplies, and CDOM sunscreen, may actually also contain the seeds of usual red tide demise, i.e., even in the absence of diatom-raised herbivores within slope intrusions.

[52] Given a choice of alternative food, most shelf copepods do not ingest *K. brevis*, but some will, for example, *Acartia tonsa*, if the toxic prey is present in high enough numbers [*Turner et al.*, 1998]. During the October 1999 red tide of ~30 ug chl L^{-1} off Sarasota, both *Temora turbinada* and *Centropages velificatus* also appeared to eat *K. brevis*, with cells found in their mouths. Using an October 1999 stock of 4 ug dw L^{-1} of just *A. tonsa* above the 10-m isobath off Tampa Bay, a P/B ratio of ~0.5 [*Heinle*, 1966], a gross growth efficiency of ~0.15 [*Marshall*, 1973], a C/dw ratio of ~0.5 [*Parsons et al.*, 1984], and a C/chl ratio of ~30 for *K. brevis* [*Shanley and Vargo*, 1993], their grazing stress could have removed ~13.3 ug chl L^{-1} of red tide over the next 60 days, passing brevitoxins to the higher trophic levels [*Tester et al.*, 2000]. During ECOHAB surveys, the mean stock of *K. brevis* along this isobath in October 1999 was 13.7 ug chl L^{-1}; it declined to 0.03 ug chl L^{-1} by December 1999.

[53] Since the mean near-surface flows at the ECOHAB arrays on the 10-m isobath were also offshore in an upwelling pattern during most of October–December 1999, as simulated in October–November 1998 (Figure 15), however, we do not yet know if the decline of the larger 1999 red tide was due to consumption by herbivores and/or offshore export by currents. The fate of these 1998–1999 red tides and others thus remains the subject of the next set of simulation analyses from our coupled biophysical models. We must now add explicit representation of both estuarine and sediment sources of phosphorus, nitrogen fixers, CDOM loadings, and frontal aggregations.

[54] However, we are pleased that a combination of cases 1 and 2 of the present model replicated field data on slope water intrusions of nitrate and silicate, regeneration of ammonium, light penetration, phytoplankton partition of primary production, grazing stresses, and carbon dioxide emissions on the WFS. Except under unrealistically persistent CDOM stocks, the deep sea intrusions were not a recipe for red tide initiation off central Florida, between Tampa and Fort Myers, where harmful algal blooms have occurred 24 out of the last 25 years. Any future monitoring system must now deal with more complex local sources of nutrients, of CDOM, of phytoplankton seed populations, and of selective herbivores, all focused at convergence fronts, to specify initial conditions for operational forecasts of the onset and duration of WFS red tides.

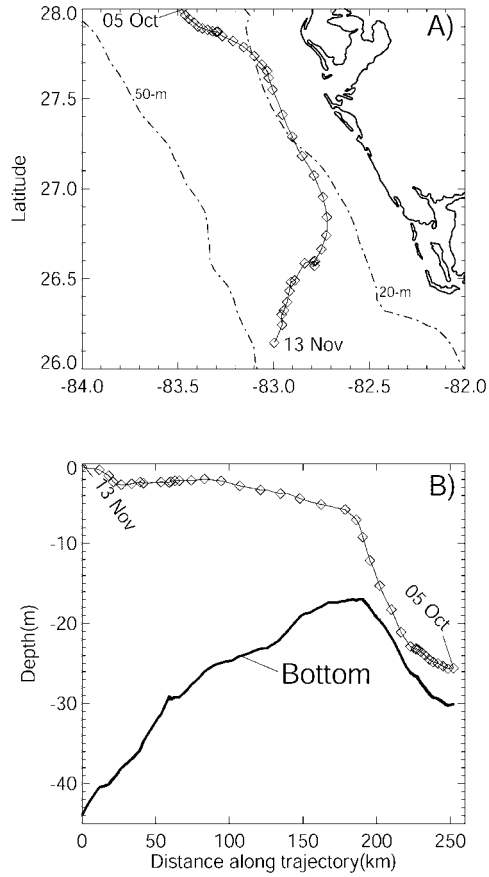

Figure 15. The daily three-dimensional trajectory (open diamonds) of neutrally buoyant microflagellates during 5 October to 13 November 1998 with respect to (a) location of the water parcel and (b) depth during transit. During maximal upwelling at ~4 m d^{-1} the innocula of settling diatoms and migrating *K. brevis* would have the greatest probability of retention within the parcel.

Appendix A

[55] In our simple biological model, the carbon-based growth of diatoms required nitrate and silicate in a constant atomic ratio of 100 C/15 N/15 Si [*Brzezinski*, 1985]. Their assumed C/chl weight ratio of 50, instead of the one of ~200 found for all particulate matter during the NEGOM and ECOHAB cruises [*Jochens and Nowlin*, 1999; *Heil et al.*, 2002], yielded a particulate PN/chl ratio (umol/ug) of ~0.6, as measured during diatom blooms [*Walsh et al.*, 1978]. Finally, a composite chlorophyll content of ~0.5 ×

10^{-5} ug chl cell^{-1} implied a mixed diatom population of 90% small (8 um) and 10% large (50 um) forms of netplankton [*Walsh et al.*, 2001], with a maximal growth rate of ~2.2 d^{-1} at 30°C (Table 2).

[56] The second functional group of small flagellates of 6–8 um size, a C/chl ratio of ~100, and a chlorophyll content of ~0.5 × 10^{-6} ug chl cell^{-1} (Table 2) had a similar maximal growth rate of diatoms, i.e., ~1.8 d^{-1} at 30°C. Selective grazing losses thus determined the initial outcome of their competition, until Si limitation prevailed in the model. When diatoms are present, copepods actively select this food item on the West Florida Shelf [*Kleppel et al.*, 1996], whereas the mean grazing loss of smaller flagellates to microzooplankton is ~82% of their realized growth rate [*Fahnenstiel et al.*, 1995] and the larger diatoms suffer less predation by ciliates [*Strom and Strom*, 1996]. Since few data were available on copepod biomass in 1998 [*Sutton et al.*, 2001], we imposed grazing stresses on mainly diatoms, but not on *K. brevis* [*Turner and Tester*, 1997], as a function of their production. Flagellate losses to protozoans were a function of just the prey biomass (Table 2).

[57] In contrast, *K. brevis* had a maximal growth rate of only ~0.8 d^{-1} [*Walsh et al.*, 2001] at 30°C in our model, with a larger cellular content of ~1.0 × 10^{-5} ug chl cell^{-1} (Table 2), reflecting their shade adaptation [*Walsh et al.*, 2002]. *K. brevis* can utilize urea, vitamins, amino acids, and other forms of organic nitrogen at varying rates [*Baden and Mende*, 1979; *Shimizu and Wrensford*, 1993], providing a possible niche for these and other dinoflagellates [*Dennison and Abal*, 1999; *Glibert and Terlizzi*, 1999]. Since, the amounts of the two forms of recycled nitrogen were similar on the West Florida Shelf (Figures 6a and 6b), and the half-saturation constant for NH_4 uptake by *K. brevis* [*Steidinger et al.*, 1998] of 0.5 umol N kg^{-1} (Table 2) was the same as that for urea, we used just the former to represent autocthonous nitrogen of the model, in which all three groups consumed ammonium.

[58] With selection of the highest half-saturation rate of 1.05 umol N kg^{-1} for uptake of nitrate by diatoms (Table 2), we forced this group to be a neritic form, instead of an oligotrophic one with k_{NO_3} of <0.03 umol N kg^{-1} [*Harrison et al.*, 1996]. Diatoms had low affinity for ammonium in our model as well. Given the low-saturation light intensity of 14.8 W m^{-2} for *K brevis*, it had a competitive advantage under high CDOM, but a disadvantage in conditions of little light attenuation. Finally, *K. brevis* migrated vertically, in response to a light cue [*Walsh et al.*, 2002], diatoms aggregated and settled as a function of their biomass [*Walsh and Dieterle*, 1994], and the flagellates were neutrally buoyant.

[59] The state equations of the biological model were solved over the curvilinear horizontal grid of the POM [*He and Weisberg*, 2002, 2003; *Weisberg and He*, 2003]. In the vertical dimension, this embedded model was partitioned into a water column of 20 layers of variable depth, d, and a benthic layer of well-mixed, 5-cm thick sediments. The state variables were: diatoms (P_d) microflagellates (P_f), *K. brevis* (P_b), siliceous fecal pellets (Z_d) of copepod origin, non-siliceous fecal pellets (Z_f) of protozoan and copepod origin, ammonium (NH_4), nitrate (NO_3), silicate (SiO_4), and dissolved inorganic carbon (DIC).

[60] The processes affecting their change with time, t, were expressed in sigma coordinates by

$$\frac{\partial dP_d}{\partial t} = Tr(dP_d) - \frac{\partial}{\partial \sigma}(w_d P_d) + d g_d P_d - d\gamma_d G_d \tag{A1}$$

$$\frac{\partial dP_f}{\partial t} = Tr(dP_f) + d(g_f - \phi)P_f \tag{A2}$$

$$\frac{\partial dP_b}{\partial t} = Tr(dP_b) - \frac{\partial}{\partial \sigma}(w_b P_b) + d g_b P_b - d\gamma_b G_b \tag{A3}$$

$$\frac{\partial dZ_d}{\partial t} = Tr(dZ_d) - \frac{\partial}{\partial \sigma}(w_{zd} Z_d) + d[(1-\varepsilon_d)\gamma_d G_d - \alpha_d Z_d] \tag{A4}$$

$$\frac{\partial dZ_f}{\partial t} = Tr(dZ_f) - \frac{\partial}{\partial \sigma}(w_{zf} Z_f) + d\left[(1-\varepsilon_f)\phi P_f + (1-\varepsilon_d)\gamma_b G_b - \alpha_f Z_f\right] \tag{A5}$$

$$\frac{\partial dNH_4}{\partial t} = Tr(dNH_4) + d\left[\left(\frac{N}{C}\right)_r \cdot \left[\varepsilon_d\gamma_d G_d - g_{dNH_4} P_d + \varepsilon_d\gamma_b G_b - g_{bNH_4} P_b + (\varepsilon_f\phi - g_{fNH_4})P_f + \alpha_d Z_d + \alpha_f Z_f\right] - X_1\right] \tag{A6}$$

$$\frac{\partial dNO_3}{\partial t} = Tr(dNO_3) - d\left[\left(\frac{N}{C}\right)_r (g_{dNO_3} P_d + g_{fNO_3} P_f + g_{bNO_3} P_b) - X_1\right] \tag{A7}$$

$$\frac{\partial dSiO_4}{\partial t} = Tr(dSiO_4) + d\left[\left(\frac{Si}{C}\right)_r (\varepsilon_d\gamma_d G_d - g_d P_d) + \beta\left(\frac{Si}{C}\right) Z_d\right] \tag{A8}$$

$$\frac{\partial dDIC}{\partial t} = Tr(dDIC) + d[\varepsilon_d\gamma_d G_d - g_d P_d + \varepsilon_d\gamma_d G_b - g_b P_b + (\varepsilon_f\phi - g_f)P_f + \alpha_d Z_d + \alpha_f Z_f] \tag{A9}$$

where the subscript "r" referred to the Redfield ratios of nitrogen and silicon to carbon. The "Tr(.)" terms represented physical advective and diffusive transport; the advective transport was

$$Tr(dB)_{adv} = -\frac{1}{h_1 h_2}\left[\frac{\partial}{\partial \xi}(h_2 u dB) + \frac{\partial}{\partial \varsigma}(h_1 v dB) + h_1 h_2 \frac{\partial}{\partial \sigma}(\omega B)\right] \tag{A10}$$

and diffusive transport was

$$Tr(dB)_{diff} = \frac{\partial}{\partial \sigma}\left(\frac{K_h}{d}\frac{\partial B}{\partial \sigma}\right) \tag{A11}$$

where B was any of the nine state variables above. Because of the strong implicit horizontal diffusion in the numerical algorithm for advective transport, we ignored explicit horizontal turbulent mixing, considering only the vertical component.

[61] The carbon to silicate ratio of the siliceous fecal pellets, Z_d, was not fixed, like the Redfield ratios of the phytoplankton, but instead changed because of dissolution of particulate silicon [*Marinelli et al.*, 1998]. This changing ratio was modeled by the following auxiliary equation for the ingested particulate silicon, M_{Si}.

$$\frac{\delta M_{si}}{\delta t} = \left[\sum\left(\frac{Si}{C}\right)F(Z_d)_{adv} + \sum\left(\frac{Si}{C}\right)F(Z_d)_{diff} + \sum\left(\frac{Si}{C}\right)F(Z_d)_{sink}\right]/V + \left(\frac{Si}{C}\right)_r \varepsilon_d \gamma_d P_d - \beta M_{si} \quad \text{(A12)}$$

where $F(Z_d)_{adv}$, for example, represented the mass flux of Z_d at a numerical cell interface due to advection, which was multiplied by the silicate to carbon ratio of the incoming or outgoing flux, and the summation was over the six interfaces of the cell around each grid mesh. For the diffusive and sinking fluxes $F(Z_d)_{diff}$, and $F(Z_d)_{sink}$, the summation was over just the upper and lower interfaces. The quantity V in the above expression was cell volume.

[62] Within the sediment layer, equations (A1)–(A5) reduced to

$$\frac{\partial B_i}{\partial t} = K_b \frac{\partial^2 B_i}{\partial z_s^2} - \lambda_i B_i \quad \text{(A13)}$$

where B_i was P_d, P_f, P_b, Z_d, or Z_f, λ_i was the degradation rate, and the bioturbation coefficient, K_b was a function of bottom temperature [*Walsh and Dieterle*, 1994], supplied by the POM.

[63] Equations (A6)–(A9) and (A12) for the remaining state variables instead became

$$\frac{\partial NH_4}{\partial t} = \left(\frac{N}{C}\right)_r \sum_i \lambda_i B_i + K_m \frac{\partial^2 NH_4}{\partial z_s^2} - X_{1s} \quad \text{(A14)}$$

$$\frac{\partial NO_3}{\partial t} = K_m \frac{\partial^2 NO_3}{\partial z_s^2} + X_{1s} \quad \text{(A15)}$$

$$\frac{\partial SIO_4}{\partial t} = K_m \frac{\partial^2 SIO_4}{\partial z_s^2} + \beta_s M_{si} \quad \text{(A16)}$$

$$\frac{\partial DIC}{\partial t} = \sum_i \lambda_i B_i + K_m \frac{\partial^2 DIC}{\partial z_s^2} \quad \text{(A17)}$$

$$\frac{\delta M_{si}}{\delta t} = \left(K_b \frac{Si}{C}\frac{\partial Z_d}{\partial z_s}\right)_d - \left(K_b \frac{Si}{C}\frac{\partial Z_d}{\partial z_s}\right)_{d+d_s} - \beta_s M_{si} \quad \text{(A18)}$$

where K_m was the pore water molecular diffusivity [*Fanning and Pilson*, 1974]. No microbiota utilized nutrients, unlike the previous WFS model [*Darrow et al.*, 2003], allowing a maximum return of recycled nutrients to the water column for possible use by *K. brevis*.

[64] The phytoplankton growth terms in equations (A1)–(A3) and (A6)–(A9) were given by

$$g_i = \min\left[c_i \frac{L(t,z)}{L_{is}} \exp\left(1 - \frac{L(t,z)}{L_{is}}\right), g_{i,N}, g_{i,sio_4}\right] \quad \text{(A19)}$$

$$g_{i,N} = c_i \max\left[\frac{NO_3}{k_{iNO_3} + NO_3}, \frac{NH_4}{k_{iNH_4} + NH_4}\right] \quad \text{(A20)}$$

$$g_{i,SIO_4} = c_i \frac{SIO_4}{k_{iSIO_4} + SIO_4} \quad \text{(A21)}$$

where subscript "i" was d, f, or b for diatoms, microflagellates, and *K. brevis*, respectively. The maximum growth rates, c_i, were a function of the 3-D temperature fields computed by the POM and doubled for every 10°C increase. The half saturation constants, k_{iNO_3}, k_{iNH_4}, and k_{iSIO_4}, for nutrient uptake by the three algal groups are given in Table 2.

[65] The light field was calculated [*Fasham et al.*, 1983; *Taylor et al.*, 1991] as a function of time of day, assuming a sinusoidal distribution over the photoperiod by

$$L(t,z) = I_m \sin(\pi t_s/\Delta)\left[R_b e^{-(k_b + CDM)z} + (1 - R_b)e^{-k_r z}\right]e^{-k_c z} \quad \text{(A22)}$$

where t_s was time since sunrise, Δ the photoperiod, $0 < t_s/\Delta < 1$, k_b and k_r were the respective attenuations by water of blue (443 nm) and red (670 nm) wavelengths [*Paulson and Simpson*, 1977], R_b was the fraction of blue surface light, and z was depth below the sea surface, with

$$k_c = \frac{1}{z}\int_0^z \left(k_d P_d + k_f P_f + k_b P_b\right)dz \quad \text{(A23)}$$

$$I_m = 24 I_p(\pi/2\Delta) \quad \text{(A24)}$$

The daily mean PAR, I_p, constant over the shelf, was calculated from NCEP data [*Kistler et al.*, 2001] as 50% of the 1998 monthly average of net surface shortwave fluxes at 27.6°N, 82.5°W. CDM was the attenuation at 443 nm of CDOM, computed from the POM's salinity field, while the values of k_b and k_r were those of oceanic waters, not those of coastal CDOM-impacted ones.

[66] The products of the specific grazing rates on diatoms and *K. brevis*-gamma$_{d,F}$ - and the grazer abundances G_d and G_b were actually specified as a fraction of the previous day's production (Table 2) since no time series of herbivore abundance was available for most of 1998: 90% for diatoms and 10% for the toxic dinoflagellates, respectively. If the average water column concentration of diatoms exceeded 10 ug chl L^{-1}, the grazing loss was then set to100% of the net photosynthesis in an attempt to mimic density-dependent mortality. The fraction of microflagellate biomass grazed per

day was instead only a function of the microflagellate standing stock, where a grazing coefficent of 0.075 was based upon sensitivity analyses of the model. In terms of the fate of grazed phytoplankton, 85% was respired to the CO_2 pool of the DIC, with 15% egested as fecal pellets [*Walsh et al.*, 1999].

[67] The nitrification rate was modeled using a Michaelis-Menten expression:

$$X_1 = 0.04\left(\frac{NH_4}{k_{NIT} + NH_4}\right) \tag{A25}$$

where 0.04 umole N Kg^{-1} d^{-1} was the maximum rate. Within the sediment layer, the nitrification rate was half the degradation rate [*Florek and Rowe*, 1983], i.e.,

$$X_{ls} = 0.5\left(\frac{N}{C}\right)_r \sum_i \lambda_i B_i \tag{A26}$$

[68] A no-flux boundary condition was imposed along solid coastal boundaries. At the open boundaries (cross shelf off Mobile Bay and off the Florida Keys and along shelf at the 200-m isobath) time-dependent nitrate, ammonium, and silicate values were prescribed at inflow points using the NEGOM/ECOHAB cruises. Initial conditions were interpolated fields from the May 1998 NEGOM/MOTE cruises.

[69] In the height coordinate, the vertical velocity in Tr_{adv} and the settling velocities w_b, w_d, w_{zd}, and w_{zf} were identically zero at the air-sea and water-sediment interfaces. The diffusive fluxes were also set to zero at the air-sea interface in equations (A1)–(A8), whereas for equation (A9) it was described by

$$\left(\frac{K_h}{d}\frac{\partial DIC}{\partial \sigma}\right)_0 = 1.11 \times 10^{-5} W \alpha \left[(pCO_2)_{air} - (pCO_2)_0\right] \tag{A27}$$

where W was a constant wind speed of 5 m s^{-1} and alpha was the solubility of CO_2 in seawater. The partial pressure of CO_2 in air $(pCO_2)_{air}$ was assumed to be 365 uatm. In the top layer of the water column, $(pCO_2)_0$ and alpha were calculated [*Peng et al.*, 1987] as a function of POM's temperature and salinity, using alkalinity = 520 + 51.2 salinity [*Millero et al.*, 1998].

[70] At the water-sediment interface, the boundary conditions of all state variables were

$$\left(\frac{K_h}{d}\frac{\partial B}{\partial \sigma}\right)_d = \left(K_{b,m}\frac{\partial B}{\partial z_s}\right)_d \tag{A28}$$

At the bottom of the sediment layer, all of the fluxes were zero.

[71] **Acknowledgments.** This analysis was funded by grants NA76RG0463 and NA96OP0084 from the National Oceanic and Atmospheric Administration to JJW, GAV, and RHW, R 827085-01-0 from the Environmental Protection Agency to GAV, NAG5-6449 to JJW and NAS5-97128 to FMK from the National Aeronautics and Space Administration, OCS 99-0051 to FMK, 1435-0001-30804 to RHW, and 1435-01-97-CT-30851 to AEJ and DCB from the Minerals Management Service, as well as N00014-96-1-5024 to KAF, N00014-99-1-0212 to JJW, and N00014-98-1-0158 to RHW from the Office of Naval Research. We also thank the State of Florida for support of JJW, GAV, GJK, FMK, KAF, and RHW and Fred Lipschultz for the del^{15}PON data. This is ECOHAB contribution 55.

References

Altabet, M. A., and J. J. McCarthy, Temporal and spatial variations in the natural abundance of $\delta^{15}N$ in PON from a warm-core ring, *Deep Sea Res.*, *32*, 755–772, 1985.

Aminot, A., and R. Kerovel, Dosage automatique de l'uree dans l'ea de mer: Une methode tres sensible a la diacelyl mnoixme, *Can. J. Fish. Aquat. Sci.*, *39*, 174–183, 1982.

Andrews, S. S., S. Caron, and O. C. Zafiriou, Photochemical oxygen consumption in marine waters: A major sink for colored dissolved organic matter?, *Limnol. Oceanogr.*, *45*, 267–277, 2000.

Atlas, E. L., L. I. Gordon, S. W. Hager, and P. K. Park, A practical manual for use of the Technicon AutoAnalyzer in seawater nutrient analysis (revised), *Tech. Rep. 215*, pp. 1–49, Dep. of Oceanogr., Oregon State Univ., Corvallis, 1971.

Austin, H. M., and J. I. Jones, Seasonal variation of physical oceanographic parameters on the Florida Middle Ground and their relation to zooplankton biomass on the West Florida Shelf, *Fla. Sci.*, *37*, 16–32, 1974.

Baden, D. G., and T. J. Mende, Amino acid utilization by *Gymnodinium breve*, *Phytochemistry*, *18*, 247–251, 1979.

Brzezinski, M. A., The Si:C:N ratio of marine diatoms: Interspecific variability and the effect of some environmental variables, *J. Phycol.*, *2*, 347–357, 1985.

Carder, K. L., and R. G. Steward, A remote-sensing reflectance model of a red-tide dinoflagellate off west Florida, *Limnol. Oceanogr.*, *30*, 286–298, 1985.

Carder, K. L., R. G. Steward, G. R. Harvey, and P. B. Ortner, Marine humic and fulvic acids: Their effects on remote sensing of ocean chlorophyll, *Limnol. Oceanogr.*, *34*, 68–81, 1989.

Carder, K. L., F. R. Chen, Z. P. Lee, S. K. Hawes, and D. Kamykoski, Semianalytic Moderate-Resolution Imaging Spectrometer algorithms for chlorophyll a and absorption with bio-optical domains based on nitrate-depletion temperatures, *J. Geophys. Res.*, *104*, 5403–5421, 1999.

Corbett, D. R., J. Chanton, W. Burnett, K. Dillon, and C. Rutkowski, Patterns of groundwater discharge into Florida Bay, *Limnol. Oceanogr.*, *44*, 1045–1055, 1999.

Curl, H., The hydrography and phytoplankton ecology of the inshore, northeastern Gulf of Mexico, *Publ. Inst. Mar. Sci. Univ. Tex.*, *6*, 278–320, 1959.

Darrow, B. P., R. T. Masserini, G. A. Vargo, and J. J. Walsh, An analysis of factors effecting the growth of benthic microalgae following a phytoplankton bloom on the West Florida shelf, *Cont. Shelf Res.*, in press, 2003.

Del Castillo, C. E., F. Gilbes, P. G. Coble, and F. E. Muller-Karger, On the dispersal of riverine dissolved organic matter over the West Florida Shelf, *Limnol. Oceanogr.*, *45*, 1425–1432, 2000.

Dennison, W. C., and E. G. Abal, *Moreton Bay Study: A Scientific Basis for the Healthy Waterways Campaign*, 246 pp., S. E. Queensland Reg. Water Qual. Manage. Strategy, Brisbane, 1999.

Fahnenstiel, G. L., M. J. McCormick, G. A. Lang, D. G. Redalje, S. E. Lohrenz, M. Markowitz, B. Wagoner, and H. J. Carrick, Taxon-specific growth and loss rates for dominant phytoplankton populations from the northern Gulf of Mexico, *Mar. Ecol. Prog. Ser.*, *117*, 229–239, 1995.

Fanning, K. A., and M. E. Pilson, The diffusion of dissolved silica out of deep-sea sediments, *J. Geophys. Res.*, *79*, 1293–1297, 1974.

Fasham, M. J., P. M. Holligan, and P. R. Pugh, The spatial and temporal development of the spring phytoplankton bloom in the Celtic Sea, April 1979, *Prog. Oceanogr.*, *12*, 87–145, 1983.

Florek, R. J., and G. T. Rowe, Oxygen consumption and dissolved inorganic nutrient production in marine coastal and shelf sediments of the Middle Atlantic Bight, *Int. Rev. Gesamten. Hydrobiol.*, *68*, 73–112, 1983.

Fryer, H. D., and A. I. Aly, Nitrogen-15 variations in fertilizer nitrogen, *J. Environ. Qual.*, *2*, 317–327, 1974.

Gilbes, F., F. E. Muller-Karger, and C. E. Del Castillo, New evidence for the West Florida Shelf plume, *Cont. Shelf Res.*, *22*, 2479–2496, 2002.

Glibert, P. M., and D. E. Terlizzi, Co-occurrence of elevated urea levels and dinoflagellate blooms in temperate estuarine aquaculture ponds, *Appl. Environ. Microbiol.*, *65*, 5594–5596, 1999.

Gordon, H. R., Diffuse reflectance of the ocean: Influence of nonuniform phytoplankton pigment profile, *Appl. Opt.*, *31*, 2116–2129, 1992.

Gordon, L. I., J. C. Jennings, A. A. Ross, and J. M. Krest, A suggested protocol for continuous flow automated analyses of seawater nutrients (phosphate, nitrate, nitrite, and silicic acid) in the WOCE Hydrographic Program and the Joint Global Ocean Fluxes Study, in *WOCE Operations Manual*, vol. 3, *WHP Off. Rep. WHPO 91-1, WOCE Rep. 68/91*, pp. 1–120, U. S. World Ocean Circ. Exp. Off., College Station, Tex., 1994.

Haddad, K. D., and K. L. Carder, Ocean intrusion: One possible initiation mechanism of red tide blooms on the west coast of Florida, in *Toxic Dinoflagellate Blooms*, edited by D. L. Taylor and H. H. Seliger, pp. 269–274, Elsevier Sci., New York, 1979.

Harrison, W. G., L. R. Harris, and B. D. Irwin, The kinetics of nitrogen utilization in the oceanic mixed layer: Nitrate and ammonium interactions at nanomolar concentrations, *Limnol. Oceanogr.*, *41*, 16–32, 1996.

Harvey, G. R., D. A. Boran, L. A. Chesal, and J. N. Takar, The structure of marine fluvic acid and humic acids, *Mar. Chem.*, *12*, 119–133, 1983.

He, R., and R. H. Weisberg, The circulation and temperature budget on the west Florida continental shelf during the 1999 spring transition, *Cont. Shelf Res.*, *22*, 719–748, 2002.

He, R., and R. H. Weisberg, A Loop Current intrusion case study on the West Florida Shelf, *J. Phys. Oceanogr.*, *33*, 465–477, 2003.

Heil, C. A., G. A. Vargo, D. N. Spence, M. B. Neely, R. Merkt, K. M. Lester, and J. J. Walsh, Nutrient stoichiometry of a Gymnodinium breve bloom: What limits blooms in oligotrophic environments?, in *Proceedings of the IX International Symposium on Harmful Algal Blooms, Hobart, Australia*, edited by G. M. Hallegraeff et al., pp. 165–168, U.N. Educ., Sci., and Cult. Org., Paris, 2002.

Heinle, D. R., Production of a calanoid copepod *Acartia tonsa* in the Patuxet River estuary, *Chesapeake Sci.*, *7*, 59–74, 1966.

Hitchock, G. L., G. A. Vargo, and M. L. Dickson, Plankton community composition, production, and respiration in relation to dissolved inorganic carbon on the West Florida Shelf, April 1996, *J. Geophys. Res.*, *105*, 6579–6589, 2000.

Hopkins, T. L., The plankton of the St. Andrews Bay system, Florida, *Publ. Inst. Mar. Sci. Univ. Tex.*, *11*, 12–64, 1966.

Hu, C., F. E. Muller-Karger, D. C. Biggs, K. L. Carder, B. Nababan, D. Nadeau, and J. Vanderbloemen, Comparison of ship and satellite bio-optical measurements on the continental margin of the NE Gulf of Mexico, *Int. J. Remote Sens.*, in press, 2003.

Iverson, R. L., and H. F. Bittaker, Seagrass distribution and abundance in eastern Gulf of Mexico coastal waters, *Estuarine Coastal Shelf Sci.*, *22*, 577–602, 1986.

Jochens, A. E., and W. D. Nowlin, Northeastern Gulf of Mexico chemical hydrography and hydrography study, in *Annual Report: Year 2, OCS Study MMS 99-0054*, pp. 1–123, New Orleans, La., 1999.

Jolliff, J. K., et al., Dispersal of the Suwannee River plume over the West Florida shelf: Simulation and observation of the optical and biochemical consequences of a flushing event, *Geophys. Res. Lett.*, *30*, doi:10.1029/2003GL016964, in press, 2003.

Jones, G. B., F. G. Thomas, and C. Burdon-Jones, Influence of *Trichodesmium* blooms on cadmium and iron speciation in Great Barrier Reef lagoon waters, *Estuarine Coastal Shelf Sci.*, *23*, 387–401, 1986.

Keiber, R. J., X. Zhou, and K. Mopper, Formation of carbonyl compounds from UV-induced photodegradation of humic substances in natural waters: Fate of riverine carbon in the sea, *Limnol. Oceanogr.*, *35*, 1503–1515, 1990.

Khromov, N. S., Distribution of plankton in the Gulf of Mexico and some aspects of its seasonal dynamics, in *Soviet-Cuban Fishery Research*, edited by A. S. Bogdanov, pp. 36–56, Isr. Program for Sci, Transl., Jerasulem, 1969.

Kistler, R., et al., The NCEP-NCAR 50-year reanalysis: Monthly means CD-ROM and documentation, *Bull. Am. Meteorol. Soc.*, *82*, 247–267, 2001.

Kleppel, G. S., C. A. Burkart, K. Carter, and C. Tomas, Diets of calanoid copepods on the west Florida continental shelf: Relationships between food concentration, food composition and feeding activity, *Mar. Biol.*, *127*, 209–218, 1996.

Kourafalou, V. H., L. Y. Oey, J. D. Wang, and T. L. Lee, The fate of river discharge on the continental shelf: 1. Modeling the river plume and the inner shelf coastal current, *J. Geophys. Res.*, *101*, 3415–3434, 1996.

Kreitler, C. W., Nitrogen-isotope ratios of soils and groundwater nitrate from alluvial fan aquifers in Texas, *J. Hydrol.*, *42*, 147–170, 1979.

LaPointe, B. E., and J. O'Connell, Nutrient-enhanced growth of *Cladophora prolifera* in Harrington Sound, Bermuda: Eutrophication of a confined, phosphorus limited marine ecosystem, *Estuarine Coastal Shelf Sci.*, *28*, 347–360, 1989.

Lenes, J. M., et al., Iron fertilization and the *Trichodesmium* response on the West Florida Shelf, *Limnol. Oceanogr.*, *46*, 1261–1277, 2001.

Lester, K. M., R. Merkt, C. A. Heil, G. A. Vargo, M. B. Neely, D. N. Spence, L. Melahan, and J. J. Walsh, Evolution of a *Gymnodinium breve* (Gymnodiniales, Dinophyceae) red tide bloom on the West Florida Shelf: Relationship with organic nitrogen and phosphorus, *Proceedings of the IX International Symposium on Harmful Algal Blooms, Hobart, Australia*, edited by G. M. Hallegraeff et al., pp. 161–164, U.N. Educ., Sci., and Cult. Org., Paris, 2002.

Liu, K.-K., and I. R. Kaplan, The eastern tropical Pacific as a source of ^{15}N-enriched nitrate in seawater off southern California, *Limnol. Oceanogr.*, *34*, 820–830, 1989.

Livingston, R. J., The ecology of the Apalachicola Bay system: An estuarine profile, *U.S. Fish Wildlife Serv. FWS/OBS-82/05*, pp. 1–148, Washington, D. C., 1984.

Marinelli, R. L., R. A. Jahnke, D. B. Craven, J. R. Nelson, and J. E. Eckman, Sediment nutrient dynamics on the South Atlantic Bight continental shelf, *Limnol. Oceanogr.*, *43*, 1305–1320, 1998.

Mariotti, A., P. Germon, P. Hubert, P. Kaiser, R. Letolle, A. Tardieux, and P. Tardieux, Experimental determination of nitrogen kinetic isotope fractionation: Some principles, illustrations for denitrification and nitrification, *Plant Soil Sci.*, *62*, 413–430, 1981.

Marshal, N., Chlorophyll *a* in the phytoplankton in coastal waters of the eastern Gulf of Mexico, *J. Mar. Res.*, *15*, 14–32, 1956.

Marshall, S. M., Respiration and feeding in copepods, *Adv. Mar. Biol.*, *11*, 57–120, 1973.

Masserini, R. T., and K. A. Fanning, A sensor package for the simultaneous determination of nanomolar concentrations of nitrite, nitrate, and ammonia in seawater by fluorescence detection, *Mar. Chem.*, *68*, 323–333, 2000.

Millero, F. J., K. Lee, and M. Roche, Distribution of alkalinity in the surface waters of the major oceans, *Mar. Chem.*, *60*, 111–130, 1998.

Millie, D. F., G. J. Kirkpatrick, and B. T. Vinyard, Relating photosynthetic pigments and in vivo optical density spectra to irradiance for the Florida red tide dinoflagellate, *Gymnodinium breve*, *Mar. Ecol. Prog. Ser.*, *120*, 65–75, 1995.

Minagawa, M., and E. Wada, Nitrogen isotope ratios of red tide organisms in the East China Sea: A characterization of biological nitrogen fixation, *Mar. Chem.*, *19*, 245–259, 1986.

Muller-Karger, F. E., The spring 1998 northeastern Gulf of Mexico (NEGOM) cold water event: Remote sensing evidence for upwelling and for eastward advection of Mississippi water (or: How an errant Loop Current anticyclone took the NEGOM for a spin), *Gulf Mex. Sci.*, *18*, 55–67, 1998.

O'Donohue, M. J., C. A. Heil, S. Lowe, J. Horrocks, E. G. Abal, S. Costanzo, and W. C. Dennison, Assessing the impact of a flood event on Moreton Bay using marine plants as bioindicators of water quality, in *Moreton Bay and Catchment*, edited by I. R. Tibbetts, N. J. Hall, and W. C. Dennison, pp. 585–596, Univ. of Queensland, Brisbane, Queensl., Australia, 1998.

O'Reilly, J. E., S. Maritorena, B. G. Mitchell, D. A. Siegel, K. L. Carder, S. A. Garver, M. Kahru, and C. R. McClain, Ocean color algorithms for SeaWiFS, *J. Geophys. Res.*, *103*, 24,937–24,953, 1998.

Parsons, T. R., M. Takahashi, and B. Hargrave, *Biological Oceanographic Processes*, 50 pp., Pergamon, New York, 1984.

Paulson, C. A., and J. J. Simpson, Irradiance measurements in the upper ocean, *J. Phys. Oceanogr.*, *7*, 952–956, 1977.

Peng, T. H., T. Takahashi, W. S. Broeker, and J. Olafsson, Seasonal variability of carbon dioxide, nutrients and oxygen in the northern North Atlantic surface water: Observations and a model, *Tellus, Ser. B*, *39*, 439–458, 1987.

Shanley, E., and G. A. Vargo, Cellular composition, growth, photosynthesis, and respiration rates of *Gymnodinium breve* under varying light levels, in *Toxic Phytoplankton Blooms in the Sea*, edited by T. J. Smayda and Y. Shimizu, pp. 831–836, Elsevier Sci., New York, 1993.

Shimizu, Y., and G. Wrensford, Peculiarities in the biosynthesis of brevitoxins and metabolism of *Gymnodinium breve*, in *Toxic Phytoplankton Blooms in the Sea*, edited by T. J. Smayda and Y. Shimizu, pp. 919–923, Elsevier Sci., New York, 1993.

Slawyk, L. R., and J. J. MacIsaac, Comparison of two automated ammonium methods in a region of coastal upwelling, *Deep Sea Res.*, *19*, 521–524, 1972.

Steidinger, K. A., G. A. Vargo, P. A. Tester, and C. R. Tomas, Bloom dynamics and physiology of *Gymnodinium breve* with emphasis on the Gulf of Mexico, in *Physiological Ecology of Harmful Algal Blooms*, edited by D. M. Anderson, A. D. Cembella, and G. M. Hallegraeff, pp 135–153, Springer-Verlag, New York, 1998.

Strom, S. L., and M. W. Strom, Microplankton growth, grazing, and community structure in the northern Gulf of Mexico, *Mar. Ecol. Prog. Ser.*, *130*, 229–240, 1996.

Sutton, T., T. Hopkins, A. Remsen, and S. Burghart, Multisensor sampling of pelagic ecosystem variables in a coastal environment to estimate zooplankton grazing impact, *Cont. Shelf Res.*, *21*, 69–87, 2001.

Taylor, A. H., A. J. Watson, M. Ainsworth, J. E. Robertson, and D. R. Turner, A modeling investigation of the role of phytoplankton in the balance of carbon at the surface of the North Atlantic, *Global Bioegochem. Cycles*, *5*, 151–172, 1991.

Tester, P. A., and K. A. Steidinger, *Gymnodinium breve* red tide blooms: Initiation, transport, and consequences of surface circulation, *Limnol. Oceanogr.*, *42*, 1039–1051, 1997.

Tester, P. A., J. T. Turner, and D. Shea, Vectorial transport of toxins from the dinoflagellate *Gymnodinium breve* through copepods to fish, *J. Plankton Res.*, *22*, 47–62, 2000.

Turner, J. T., and P. A. Tester, Toxic marine phytoplankton, zooplankton grazers, and pelagic food webs, *Limnol. Oceanogr.*, *42*, 1203–1214, 1997.

Turner, J. T., P. A. Tester, and P. J. Hansen, Interactions between toxic marine phytoplankton and metazoan and protistan grazers, in *Physiological Ecologoy of Harmful Algal Blooms*, edited by D. M. Anderson, A. D. Cembella, and G. M. Hallegraeff, pp. 453–474, Springer-Verlag, New York, 1998.

Walsh, J. J., and D. A. Dieterle, CO_2 cycling in the coastal ocean. I. A numerical analysis of the southeastern Bering Sea, with applications to the Chukchi Sea and the northern Gulf of Mexico, *Prog. Oceanogr.*, *34*, 335–392, 1994.

Walsh, J. J., and K. A. Steidinger, Saharan dust and Florida red tides: The cyanophyte connection, *J. Geophys. Res.*, *106*, 11,597–11,612, 2001.

Walsh, J. J., T. E. Whitledge, F. W. Barvenik, C. D. Wirick, S. O. Howe, W. E. Esaias, and J. T. Scott, Wind events and food chain dynamics within the New York Bight, *Limnol. Oceanogr.*, *23*, 659–683, 1978.

Walsh, J. J., D. A. Dieterle, M. B. Meyers, and F. E. Muller-Karger, Nitrogen exchange at the continental margin: A numerical study of the Gulf of Mexico, *Prog. Oceanogr.*, *23*, 245–301, 1989.

Walsh, J. J., et al., A numerical simulation of carbon/nitrogen cycling during spring upwelling in the Cariaco Basin, *J. Geophys. Res.*, *104*, 7807–7825, 1999.

Walsh, J. J., B. Penta, D. A. Dieterle, and W. P. Bissett, Predictive ecological modeling of harmful algal blooms, *Hum. Ecol. Risk Assess.*, *7*, 1369–1383, 2001.

Walsh, J. J., K. D. Haddad, D. A. Dieterle, R. H. Weisberg, Z. Li, H. Yang, F. E. Muller-Karger, C. A. Heil, and W. P. Bissett, A numerical analysis of the landfall of 1979 red tide of *Karenia brevis* along the west coast of Florida, *Cont. Shelf Res.*, *22*, 15–38, 2002.

Wanninkhof, R., et al., Gas exchange, dispersion, and biological productivity on the West Florida Shelf: Results from a Lagrangian tracer study, *Geophys. Res. Lett.*, *24*, 1767–1770, 1997.

Weisberg, R. H., and R. He, Local and deep-ocean forcing contributions to anomalous water properties on the West Florida Shelf, *J. Geophys. Res.*, doi:10.1029/2002JC001407, in press, 2003.

Weisberg, R. H., B. D. Black, and H. Yang, Seasonal modulation of the west Florida continental shelf circulation, *Geophys. Res. Lett.*, *23*, 2247–2250, 1996.

Weisberg, R. H., B. Black, and Z. Li, An upwelling case study on Florida's west coast, *J. Geophys. Res.*, *105*, 11,459–11,469, 2000.

Weisberg, R. H., Z. Li, and F. E. Muller-Karger, West Florida Shelf response to local wind forcing: April 1998, *J. Geophys. Res.*, *106*, 31,239–31,262, 2001.

Wright, S. W., S. W. Jeffrey, R. F. Mantoura, C. A. Llewellyn, T. Bjornland, D. Repeta, and N. Welschmeyer, Improved HPLC method for the analysis of chlorophylls and carotenoids from marine phytoplankton, *Mar. Ecol. Prog. Ser.*, *77*, 183–196, 1991.

Yang, H., and R. H. Weisberg, Response of the West Florida Shelf circulation to climatological wind stress forcing, *J. Geophys. Res.*, *104*, 5301–5320, 1999.

Yang, H., R. H. Weisberg, P. Niiler, and A. Sturges, Lagrangian circulation and forbidden zone on the West Florida Shelf, *Cont. Shelf Res.*, *19*, 1221–1245, 1999.

D. C. Biggs and A. E. Jochens, Department of Oceanography, Texas A&M University, College Station, TX 77843, USA.

B. P. Darrow, D. A. Dieterle, K. A. Fanning, R. He, C. Hu, J. K. Jolliff, K. M. Lester, F. E. Muller-Karger, B. Nababan, T. T. Sutton, G. A. Vargo, J. J. Walsh, and R. H. Weisberg, College of Marine Science, University of South Florida, St. Petersburg, FL 33701, USA. (walsh@seas.marine.usf.edu)

G. J. Kirkpatrick, Mote Marine Laboratory, 1600 Ken Thompson Parkway, Sarasota, FL 34236, USA.